

Discovery of 2-{4-[(3*S*)-Piperidin-3-yl]phenyl}-2*H*-indazole-7-carboxamide (MK-4827): A Novel Oral Poly(ADP-ribose)polymerase (PARP) Inhibitor Efficacious in BRCA-1 and -2 Mutant Tumors

Philip Jones,* Sergio Altamura, Julia Boueres, Federica Ferrigno, Massimiliano Fonsi, Claudia Giomini, Stefania Lamartina, Edith Monteagudo, Jesus M. Ontoria, Maria Vittoria Orsale, Maria Cecilia Palumbi, Silvia Pesci, Giuseppe Roscilli, Rita Scarpelli, Carsten Schultz-Fademrecht, Carlo Toniatti, and Michael Rowley

IRBM/Merck Research Labs Rome, Via Pontina km 30,600, 00040 Pomezia, Italy

Received August 10, 2009

We disclose the development of a novel series of 2-phenyl-2*H*-indazole-7-carboxamides as poly(ADP-ribose)polymerase (PARP) 1 and 2 inhibitors. This series was optimized to improve enzyme and cellular activity, and the resulting PARP inhibitors display antiproliferation activities against BRCA-1 and BRCA-2 deficient cancer cells, with high selectivity over BRCA proficient cells. Extrahepatic oxidation by CYP450 1A1 and 1A2 was identified as a metabolic concern, and strategies to improve pharmacokinetic properties are reported. These efforts culminated in the identification of 2-{4-[(3*S*)-piperidin-3-yl]phenyl}-2*H*-indazole-7-carboxamide **56** (MK-4827), which displays good pharmacokinetic properties and is currently in phase I clinical trials. This compound displays excellent PARP 1 and 2 inhibition with $IC_{50} = 3.8$ and 2.1 nM, respectively, and in a whole cell assay, it inhibited PARP activity with $EC_{50} = 4$ nM and inhibited proliferation of cancer cells with mutant BRCA-1 and BRCA-2 with CC_{50} in the 10–100 nM range. Compound **56** was well tolerated in vivo and demonstrated efficacy as a single agent in a xenograft model of BRCA-1 deficient cancer.

Introduction

Poly(ADP-ribose) polymerase (PARP)-1 is the founding and most abundant member of poly(ADP-ribosyl)ating proteins, a family of some 18 proteins.¹ Several of the PARP^a family of enzymes share a catalytic PARP homology domain and are characterized by the ability to catalyze the transfer of ADP-ribose units to proteins using nicotinamide adenine dinucleotide (NAD^+) as the substrate, resulting in the formation of long and branched poly(ADP)ribose (PAR) chains.^{2,3} More recent characterization suggests that while PARPs 1–5 function as poly(ADP-ribosyl)ating proteins, some of the other family members may indeed be mono-ADP-ribosyltransferases and other members of the family may be catalytically inactive.^{1c} PARP-1 and the closely related PARP-2 are nuclear proteins and possess DNA binding domains.⁴ These DNA binding domains serve to localize and rapidly bind these PARPs to the sites of DNA single- and double-strand breaks (SSB and DSB, respectively). With binding at sites of lesion, the catalytic activity of these enzymes is stimulated more than 500-fold, which results in the addition of PAR chains on several proteins associated with chromatin, including

histones, p53, topoisomerases, and PARP itself, plus various DNA repair proteins.⁵ This results in chromatin relaxation and fast recruitment of DNA repair factors which access the DNA breaks and repair them by a process known as base excision repair (BER).

The knockout of PARP-1 significantly impairs repair of DNA damage following exposure to radiation or cytotoxic insult,^{6,7} with the residual PARP dependent repair activity being due to PARP-2, which contributes about 10% to nuclear PARP activity.^{4,7} Similarly, PARP 1 and 2 inhibition with small molecule inhibitors has been demonstrated to sensitize tumor cells to cytotoxic agents that induce DNA damage that would normally be repaired by BER, notably alkylating agents (like temozolomide and cyclophosphamide) and topoisomerase I poisons (irinotecan and topotecan).^{8–10} Sensitization of platins, like cisplatin and carboplatin, has also been demonstrated, as has the use of PARP inhibitors as radiopotentiators, whereby the cellular damage caused by ionizing radiation is enhanced.

In addition, hyperactivation of PARP activity has been reported, caused by excessive DNA damage following oxidative insult upon ischemia reperfusion.^{2,3} The subsequent extensive PARylation of substrates results in depletion of cellular NAD^+ pools and energy stores, leading to acute neuronal and myocardial cell death by necrosis. Indeed several classes of PARP inhibitors have already been developed¹¹ and have demonstrated efficacy in animal models of these diseases.^{2,12,13} These PARP inhibitors have also shown applicability in models of inflammation,¹⁴ cardiovascular disease,¹⁵ and neurodegenerative disorders.¹⁶

PARP-1 is also known to participate in a range of other cellular processes including regulation of apoptosis, cell

*To whom correspondence should be addressed. Current address: Department of Medicinal Chemistry, Merck Research Labs Boston, Avenue Louis Pasteur 33, Boston, MA 02115-5727. Phone: +1-617-992-2292. Fax: +1-617-992-2405. E-mail: philip_jones@merck.com.

^a Abbreviations: BER, base excision repair; BRCA, breast cancer susceptibility gene; DSB, double strand break; HLM, human liver microsomes; HR, homologous recombination; NAD^+ , nicotinamide adenine dinucleotide; PAR, poly(ADP)ribose; PARP, poly(ADP-ribose)-polymerase; RLM, rat liver microsomes; SFC, supercritical fluid chromatography; shRNA, short hairpin interfering RNA; SSB, single strand break; TANK, tankyrase; V-PARP, vault PARP; WT, wild type.

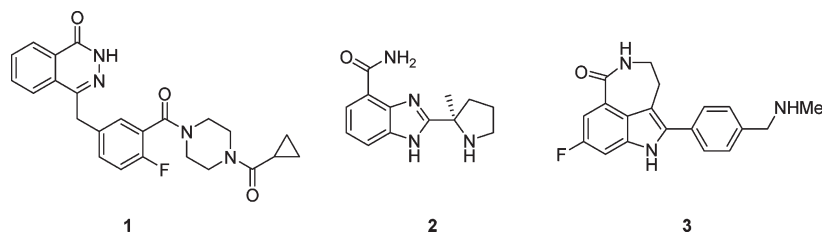


Figure 1. PARP inhibitors currently undergoing clinical trials.

division, transcriptional regulation, and differentiation, as well as chromosome stability.^{2,3} Despite PARP-1 being identified over 40 years ago, the biology of the other family members is still being elucidated,^{1,2} although PARP-4/vault PARP is known to be the catalytic component of the vault particles, which are ribonucleoprotein complexes that are involved in multidrug resistance of tumors. Tankyrases I and II are known to regulate telomere homeostasis and also to play key roles during mitotic segregation.

Recently, data have emerged suggesting that targeting more than one DNA repair pathway in tumor cells could induce “synthetic lethality”.^{17–19} Specifically, publications have appeared that described the selective killing of BRCA-1 or BRCA-2 deficient tumor cells by PARP inhibitors.^{17,18} In contrast, normal cells with an intact BRCA pathway when treated with a PARP inhibitor are viable and minimal cytotoxicity is seen. BRCA-1 and -2 are known tumor suppressors and are key components involved in the repair of DNA double strand breaks by the homologous recombination (HR) pathway, and mutations in these genes predispose individuals to hereditary breast and ovarian cancer and also prostate and pancreatic cancer.²⁰ Every day cells are faced by an onslaught of DNA damage, through metabolic processes and/or exogenous damage, and in the presence of a PARP inhibitor this attack results in persistent DNA SSB. During replication, these SSBs cause stalled replication forks and subsequently develop into DSB. In BRCA-1 and -2 deficient cells, these lesions are not repaired by the alternative DSB repair pathway of homologous recombination, resulting in gross genomic instability, cell cycle arrest, and apoptosis. Cells that are deficient in BRCA-1 and -2 have been demonstrated to be acutely sensitive to killing by PARP inhibitors in vitro and in vivo.^{17,18} In a genetically engineered mouse model for BRCA-1 associated breast cancer treatment of tumor bearing mice with the PARP inhibitor 4-[3-(4-cyclopropanecarbonylpiperazine-1-carbonyl)-4-fluorobenzyl]-2*H*-phthalazin-1-one²¹ **1** (olaparib, KU-0059436, AZD-2281) resulted in inhibition of tumor growth without signs of toxicity.²² Furthermore, clinical proof-of-concept for the use of a PARP inhibitor for the treatment of cancers with known BRCA mutations has been demonstrated, with **1** showing clinical responses in patients with breast and ovarian cancers with known BRCA 1 or 2 mutations.²³

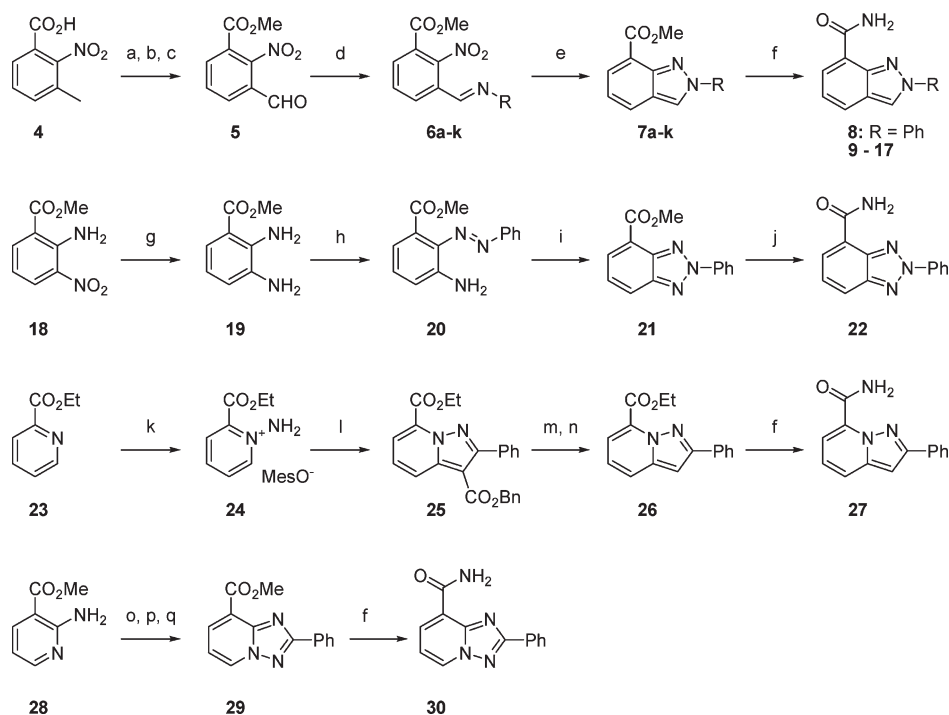
Besides **1** (Figure 1), other PARP inhibitors in clinical development include Abbott’s orally available 2-[(*R*)-2-methylpyrrolidin-2-yl]-1*H*-benzimidazole-4-carboxamide **2** (ABT-888) which is being investigated as a chemo- and radiosensitizer;²⁴ and Pfizer’s 8-fluoro-2-(4-methylaminomethylphenyl)-1,3,4,5-tetrahydroazepino[5,4,3-*cd*]indol-6-one **3** (AG014699).²⁵ Another two agents that are being investigated in the clinic are Inotek Pharmaceuticals’ INO-1001²⁶ and BiPar Science’s BS-201;²⁷ neither structure has been disclosed. The latter is currently in phase II studies for the treatment of triple-negative breast cancer.

In this article the development of a novel series of 2-phenyl-2*H*-indazole-7-carboxamides as PARP 1 and 2 inhibitors for the treatment of BRCA-1 and -2 deficient cancers is reported. The introduction of a (di)alkylaminomethyl substituent on the pendent aryl moiety of this scaffold resulted in compounds with improved cellular activity, although at the expense of metabolic liabilities in the form of extrahepatic oxidation by CYP450 1A1 and 1A2. Strategies to improve pharmacokinetic properties are reported, culminating in the discovery of 2-{4-[(3*S*)-piperidin-3-yl]phenyl}-2*H*-indazole-7-carboxamide **56** (MK-4827) which is currently in human phase I clinical trials. This compound displays excellent potency against both the PARP-1 and PARP-2 enzymes with IC₅₀ = 3.8 and 2.1 nM, respectively, and in a whole cell assay it inhibits PARP activity with EC₅₀ = 4.0 nM and EC₉₀ = 45 nM. This indazole-7-carboxamide inhibits proliferation of cancer cell lines with mutant BRCA-1 and BRCA-2 in vitro and is efficacious in xenograft models following oral dosing.

Results and Discussion

Chemistry. Synthetic routes for the preparations of diverse [6,5]-bicyclic heterocyclic systems **8**, **22**, **27**, and **30** bearing pendent primary carboxamide and phenyl groups are described in Scheme 1. Indazole PARP inhibitors were prepared from methyl 3-formyl-2-nitrobenzoate (**5**), itself available from oxidation of methyl 3-methyl-2-nitrobenzoate. Condensation with substituted anilines in refluxing EtOH gave azomethines **6a–j** that could then be treated with NaN₃ in DMF at 90 °C, and initial substitution of the ortho-nitro group and subsequent cyclization gave the corresponding indazoles **7a–j** as described by Kuvshinov.²⁸ Amide formation using ammonia in MeOH in a sealed tube furnished the desired compounds **8–17**. The 1,2,3-benzotriazole **22** was prepared from methyl 2,3-diaminobenzoate (**19**) by condensation with nitrosobenzene in AcOH to give **20**, followed by oxidation cyclization using stoichiometric Cu(OAc)₂ under an O₂ atmosphere. Functional group interconversion then yielded **22**. The synthesis of the pyrazolo-[1,5-*a*]pyridine **27** started from ethyl 2-picolinate (**23**) which upon treatment with *O*-mesitylenesulfonylhydroxylamine gave the *N*-aminopyridinium salt **24**. The key bicycle **25** was then prepared by a [3 + 2] cycloaddition of the *N*-aminopyridinium salt with an alkynoic ester.²⁹ Hydrogenation of the benzyl ester **25**, followed by decarboxylation in 48% HBr, gave the required 2-phenylpyrazolo-[1,5-*a*]pyridine-7-carboxamide (**27**) after amide formation. A similar synthetic strategy was employed for the formation of 2-phenyl[1,2,4]triazolo[1,5-*a*]pyridine-8-carboxamide (**30**), in which case the *N*-aminopyridinium salt was condensed with benzaldehyde to elaborate the key heterocyclic intermediate **29** that was subsequently transformed to **30**.³⁰

Substituted 2-arylindazole-7-carboxamides were prepared using the previously described route from the appropriately

Scheme 1^a

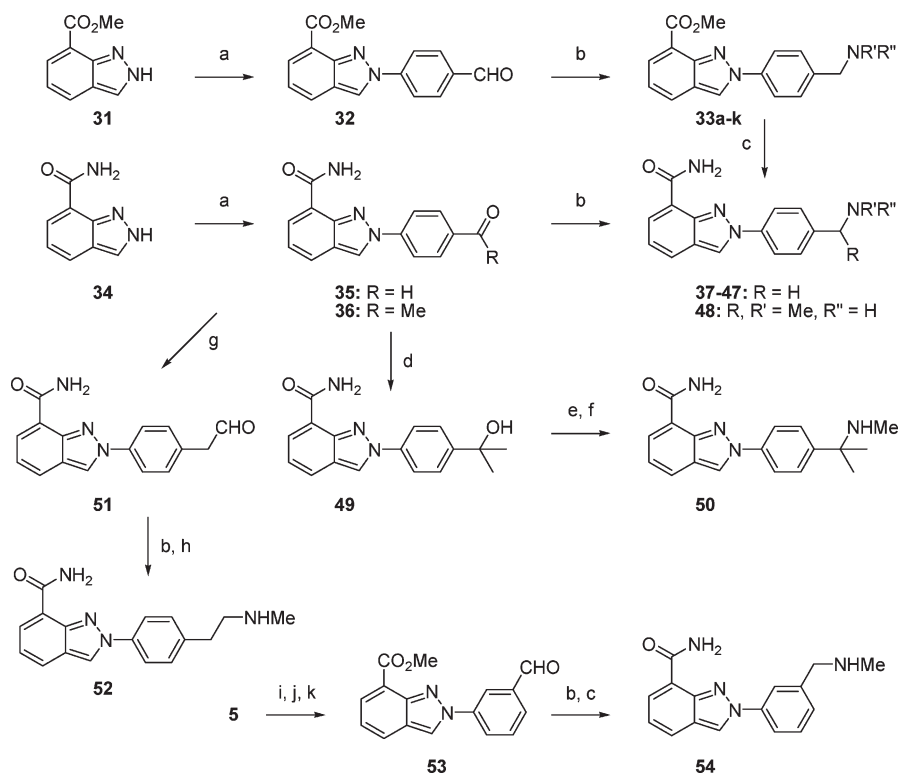
^a Reagents: (a) HCl, MeOH, Δ ; (b) NBS, (BzO)₂, CCl₄, Δ ; (c) NMMO, MeCN; (d) RNH₂, EtOH, Δ ; (e) NaN₃, DMF, 90 °C; (f) NH₃, MeOH, sealed tube, 60 °C; (g) H₂, Pd/C, MeOH; (h) nitrosobenzene, AcOH; (i) Cu(OAc)₂, O₂, DMF, 80 °C; (j) NaOH, then HATU, NH₃, DIPEA, DMF; (k) H₂N-OMes, DCM; (l) PhCCCO₂Bn, K₂CO₃, THF; (m) H₂, Pd/C, EtOH, EtOAc; (n) 48% HBr, Δ ; (o) H₂N-OMes, dioxane; (p) PhCHO, Δ ; (q) KOH, MeOH.

substituted aniline, or alternatively methyl-2*H*-indazole-7-carboxylate (**31**) and indazole-7-carboxamide (**34**) can undergo microwave assisted S_NAr substitution of *p*-fluorobenzaldehyde or fluoroacetophenone in DMF in the presence of K₂CO₃ (Scheme 2). Reductive amination using ZnCl₂ and NaBH₃(CN) together with the appropriate amines gave derivatives **37–48**. The corresponding *gem*-dimethyl analogue **50** was prepared by conversion of methyl ketone **36** to the corresponding tertiary alcohol **49**. This alcohol underwent a Ritter rearrangement to yield the corresponding formamide,³¹ which was in turn reduced to give **50**. Homologation to the corresponding phenethylamine **52** was achieved by treating aldehyde **35** with methoxymethyltriphenylphosphonium chloride and KO^tBu followed by mild acid treatment to yield phenacetaldehyde **51**, followed by reductive amination. The isomeric benzylamine **54** was prepared utilizing 3-aminobenzaldehyde ethylene acetal in the cyclization to form the indazole followed by functional group interconversion.

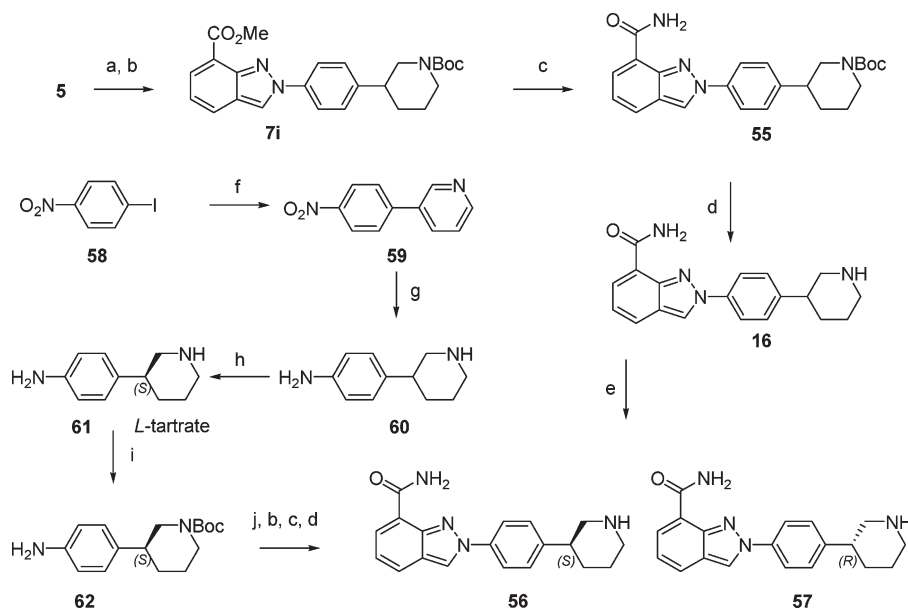
Derivatives bearing the 4-[(3*S*)-piperidin-3-yl]phenyl moiety were prepared by one of two routes illustrated in Scheme 3. Racemic *N*-Boc-3-(4-aminophenyl)piperidine was condensed with methyl 3-formyl-2-nitrobenzoate (**5**) and cyclized using NaN₃ in DMF as described previously to subsequently yield **7i**. Separation of **16** by chiral SFC gave the enantiomers **56** and **57**. Alternatively, 4-piperidin-3-ylaniline (**60**), readily available from Suzuki coupling of 1-iodo-4-nitrobenzene and pyridine-3-boronic acid followed by PtO₂ hydrogenation, was resolved using L-tartaric acid to yield the *S*-enantiomer **61** in high enantiomeric excess following four recrystallizations. Subsequent elaboration to **56** proceeded in high yield with no erosion of the stereochemistry to give **56** in 30% yield over five steps.

Biology. Given the interest in PARP-1 inhibition in a wide variety of therapeutic areas, a significant number of

industrial and academic groups have worked on developing inhibitors.¹¹ Most of inhibitors developed to date bind to the nicotinamide binding site, where they compete with the natural substrate nicotinamide adenine dinucleotide (NAD⁺). X-ray crystal structures and molecular modeling studies have indicated that the amide of nicotinamide makes three key hydrogen bonds to the hydroxyl group of Ser904 and the amide backbone of Gly863.³² Moreover, the pyridyl ring is engaged in π - π stacking with Tyr907. The majority of the inhibitors developed to date are close structural mimics of nicotinamide, and attempts to improve the affinity of these derivatives have been made by trying to lock the carboxamide group, which is usually free to rotate, into the desired anti-conformation. On the basis of this knowledge, four [6,5]-bicyclic heteroaromatic carboxamide derivatives **8**, **22**, **27**, and **30** were designed, all of which incorporate a nitrogen atom within the heteroaromatic ring to lock the carboxamide group into a six-membered intramolecular hydrogen bond. All four novel scaffolds were demonstrated to be modest PARP inhibitors, with the indazole derivative **8** with IC₅₀ = 24 nM displaying higher affinity than the benzotriazole **22**, pyrazolo[1,5-*a*]pyridine **27**, and the [1,2,4]triazolo[1,5-*a*]pyridine **30** in a PARP-1 SPA assay (Table 1). The indazole **8** was also demonstrated to inhibit PARP activity in cells, being able to inhibit the formation of PAR polymers following the induction of DNA damage with hydrogen peroxide. In HeLa cervical cancer cells **8** displayed EC₅₀ = 3.7 μ M and EC₉₀ = 6.2 μ M. The pharmacokinetics of **8** were also encouraging, displaying moderate stability in both rat and human microsomes (Cl_{int} = 123 and 138 (μ L/min)/mgP, respectively), and in vivo in rats **8** displayed acceptable plasma clearance (Cl = 30 (mL/min)/kg), volume of distribution of 1.8 L/kg, and terminal half-life of 5.1 h. This indazole also showed acceptable oral bioavailability, *F* = 41%.

Scheme 2^a

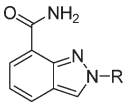
^a Reagents: (a) *p*-FC₆H₄COR, K₂CO₃, DMF, microwave; (b) R'R''NH, NaBH₃(CN), ZnCl₂, MeOH, DCE; (c) NH₃, MeOH, sealed tube, 60 °C; (d) MeMgBr, THF; (e) NaCN, H₂SO₄, DCM; (f) BH₃, THF, THF; (g) MeOCH₂P⁺Ph₃ Cl⁻, KO^tBu, Et₂O/THF, -78 °C to room temp, then HCl, Et₂O; (h) formaldehyde, NaBH₃(CN), then H₂, Pd/C, MeOH; (i) ArNH₂, EtOH, Δ; (j) NaN₃, DMF, 90 °C; (k) TFA, DCM, H₂O.

Scheme 3^a

^a Reagents: (a) ArNH₂, EtOH, Δ; (b) NaN₃, DMF, 90 °C; (c) NH₃, MeOH, sealed tube, 60 °C; (d) HCl, dioxane; (e) SFC separation; (f) 3-pyridyl-B(OH)₂, Pd(PPh₃)₄, Na₂CO₃, THF/H₂O, Δ; (g) 50 psi of H₂, PtO₂, MeOH; (h) resolution L-tartaric acid, EtOH; (i) Boc₂O, DCM; (j) 5, EtOH, Δ.

On the basis of these results, a more detailed exploration of the indazole lead **8** was undertaken in order to optimize potency, as well as pharmaceutical properties. In an effort to improve the activity, substituents were introduced at the ortho, meta, and para positions of the pendent phenyl ring, as well as the insertion of a methylene spacer between the

indazole core and the phenyl moiety. Substituents were well tolerated at the distal meta and para positions, resulting in an improvement in at least 5-fold in cellular activity, with **11** and **12** displaying EC₅₀ = 450 and 720 nM in the PARylation assay, respectively. However, substitution adjacent to the indazole was detrimental, with **10** displaying a 5-fold loss of

Table 1. In Vitro Activity of PARP Inhibitor Scaffolds^a


compd	R	PARP-1		
		IC ₅₀ (nM)	PARylation EC ₅₀ (nM)	PARylation EC ₉₀ (nM)
8	Ph	24	3700	6200
9	benzyl	130	> 5000	> 5000
10	<i>o</i> -Cl-C ₆ H ₄ -	100	ND	ND
11	<i>m</i> -Cl-C ₆ H ₄ -	14	450	5600
12	<i>p</i> -Cl-C ₆ H ₄ -	24	720	6700
22		71	ND	ND
27		55	ND	ND
30		270	ND	ND

^aValues are the mean of at least four experiments (standard deviations were within 25% of the mean values). ND = not determined.

enzyme activity, IC₅₀ = 100 nM. Similarly, homologation to the benzyl derivative **9** resulted in a similar loss of enzymatic activity.

Knowing that substitution was tolerated at the remote positions, alternative groups were introduced in the hope of picking up additional binding interactions in the adenosine binding pocket to improve the affinity and cellular activity. Efforts concentrated on the addition of polar groups with a view to improve the solubility of these lipophilic compounds, given that the prototype **8** was only sparingly soluble in phosphate buffer, 26 μg/mL.

The addition of a dimethylaminomethyl group to give **37** resulted in a 6-fold improvement in enzymatic activity, IC₅₀ = 3.7 nM, and further improved the cellular activity, inhibiting the formation of poly-ADP-ribose chains following DNA damage with EC₅₀ = 110 nM and EC₉₀ = 630 nM (Table 2). Given the submicromolar activity of this compound, its ability to inhibit the growth of cervical cancer HeLa cells where BRCA-1 had been silenced with a lentivirus expressing a short hairpin interfering RNA (shRNA) targeting BRCA-1 was tested. In parallel, the cytotoxicity against a matched pair cell line expressing an empty lentivector was also measured. In 7-day proliferation assays **37** displayed CC₅₀ = 520 nM against the BRCA-1 deficient cells and 10-fold selectivity over the BRCA-1 proficient HeLa cells where CC₅₀ = 5.6 μM, thereby confirming the previous literature reports that PARP inhibitors are capable of selectively killing BRCA-1 deficient cells.^{17,18} The addition of the basic amine also improved the physicochemical properties, with **37** displaying solubility in excess of 3 mg/mL in phosphate buffer.

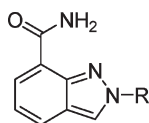
Subsequent SAR studies confirmed these results with pyrrolidine **38** and piperidine **39** displaying similar PARP inhibitory activity in vitro and in cells, inhibiting the growth of BRCA-1 silenced HeLa cells with CC₅₀ = 1.2 and 0.88 μM, respectively, and showing at least 5-fold selective cytotoxicity versus HeLa BRCA-1 wild-type cells. The less basic derivatives such as morpholine **40** displayed inferior PARP inhibition, with EC₉₀ = 6.2 μM in the PARylation assay and CC₅₀ = 5.3 μM against BRCA-1 silenced cells. Cellular activity could be improved by the incorporation of the *N*-methylpiperazine, and **41** displayed CC₅₀ = 2.7 μM in the BRCA-1 deficient cells, despite this compound displaying weaker enzyme activity, IC₅₀ = 31 nM. However, **41** showed only 3-fold selective cytotoxicity between BRCA-1

silenced and wild-type cells, suggesting some underlying toxicity. Similar micromolar activity was also seen with the trimethylethylenediamine derivative **42**, although with at least a 5-fold selectivity between BRCA-1 deficient and wild-type cells. Secondary amines were also tolerated, with the methylamine **43** displaying slightly improved activity compared to dimethylamino analogue **37** in cells, with CC₅₀ = 460 nM and more than 10-fold selectivity for BRCA-1 deficient cells. In contrast, more lipophilic ethylamine **44**, although displaying comparable enzymatic activity, was 3-fold less active in cells, and further substitution was detrimental, as the isopropylamine **47** lost both enzyme and cellular activity, with IC₅₀ = 6.7 nM and CC₅₀ = 2.0 μM in BRCA-1 deficient cells. Introduction of mono- and difluoro groups to the ethylamine, in **45** and **46**, reduced the basicity of the amine and reduced cellular activity as seen with the morpholine **40**. In general, there was good correlation between the extent of PARP inhibition in cells and the concentrations needed to inhibit growth of BRCA-1 silenced HeLa cells. In most cases EC₉₀ for inhibition of PARylation correlated with the CC₅₀ for inhibition of the proliferation of BRCA-1 silenced HeLa cells. This suggests that strong sustained PARP inhibition is required to inhibit growth in this context.

Exploration was also conducted in the isomeric series, where the methylaminomethyl group was introduced in the meta position of the phenyl ring, resulting in **54**, and although this was tolerated, inhibiting PARP activity with IC₅₀ = 5.3 nM, this derivative displayed only weak cellular activity, BRCA-1 deficient CC₅₀ = 10 μM. A loss of activity was also observed in the para regioisomer if the amine was homologated to the corresponding phenethylamine, with **52** losing almost 2 orders of magnitude in activity, PARP-1 IC₅₀ = 200 nM.

Encouraged by these results and the selective growth inhibition caused by these PARP inhibitors in BRCA-1 deficient cells, a number of compounds were profiled in microsomal stability studies and in vivo in rats (Table 3). The dimethylamino derivative **37** displayed relatively high turnover in rat liver microsomes (RLM), Cl_{int} = 177 (μL/min)/mgP, and in vivo high plasma clearance was observed in rats, in excess of hepatic blood flow. In contrast, the monomethylamine **43** showed improved stability in vitro (RLM Cl_{int} = 28 (μL/min)/mgP), yet in vivo in rats similar high plasma clearance was measured, Cl = 220 (mL/min)/kg. The plasma clearance value in excess of rat liver blood flow suggested extrahepatic metabolism. Similar observations were seen with the piperidine **39** and the isopropyl **47** derivatives, all of which displayed good stability in rat liver microsomes but plasma clearances in excess of 100 (mL/min)/kg in vivo in rats. Plasma stability studies were conducted on a number of derivatives, and no metabolism was seen in rat or human plasma. Furthermore, blood/plasma partitioning experiments revealed B/P ratios in the range 1.2–1.6, thereby failing to explain the blood clearance in excess of hepatic blood flow.

A [³H]-radiolabeled version of **43** was prepared³³ and administered iv to rats, and 80% of the radioactivity was recovered in the urine and bile within 24 h of dosing, being equally distributed between the two fluids (Figure 2). In urine, one significant metabolite was detected corresponding to the benzoic acid **63**, probably arising from oxidation of the benzylic position to the corresponding aldehyde **35** followed by further oxidation to the carboxylic acid. In contrast, in

Table 2. In Vitro Activity and Antiproliferation Activity of 2-Phenyl-2H-indazole-7-carboxamide PARP Inhibitors^a

#	R	PARP-1 IC ₅₀ (nM)	PARylation EC ₅₀ (nM)	PARylation EC ₉₀ (nM)	BRCA1- CC ₅₀ (nM)	BRCA1WT CC ₅₀ (nM)
37		3.7	110	630	520	5600
38		4.8	94	450	1200	8100
39		1.9	180	970	880	5800
40		17	1200	6200	5300	>20000
41		31	1100	2700	2700	7900
42		5.9	170	4400	3900	>20000
43		3.8	68	740	460	5400
44		4.3	150	2100	1600	7400
45		2.1	>5000	ND	ND	ND
46		14	3400	7600	>6600	>6600
47		6.7	700	2000	2000	10000
48		3.7	58	680	3100	14000
50		16	110	900	920	5500
52		200	ND	ND	19000	>20000
54		5.3	ND	ND	10300	>20000
13		2.2	46	310	130	2200

Table 2. Continued

#	R	PARP-1 IC ₅₀ (nM)	PARylation EC ₅₀ (nM)	PARylation EC ₉₀ (nM)	BRCA1- CC ₅₀ (nM)	BRCA1WT CC ₅₀ (nM)
14		1.4	13	140	270	5400
15		3.1	31	430	190	10000
16		3.2	24	220	72	2000
17		9	ND	ND	410	4500
56		3.2	4.0	45	33	860
57		2.4	30	280	470	5700

^a Values are the mean of at least four experiments (standard deviations were within 25% of the mean values).

Table 3. In Vitro and in Vivo Pharmacokinetic Parameters for 2-Phenyl-2H-indazole-7-carboxamide PARP Inhibitors

compd	RLM Cl _{int} (μL/min)/ mgP)	HLM Cl _{int} (μL/min)/ mgP)	CYP1A1 Cl _{int} (μL/min)/ mgP)	rat Cl (mL/min)/ kg)	F (%)
8	123	138	ND	30	41
37	177	1	8.7	450	
39	29	3	3.8	107	
41	34	2	<0.1	8	11
43	28	3	6	220	23
47	18	1	0.8	131	
54	32	5	5.4	69	
48	9	1	2.2	58	
50	11	<1	0.4	30	
13	52	4	0.7	87	
14	36	3	0.7	30	22
15	22	4	2.5	ND	
16	11	1	0.3	47	74
17	15	5	<0.1	ND	
56	16	4	0.3	28	65
57	7	3	<0.1	24	47

bile, both the carboxylic acid **63** and the corresponding glucuronide **64** were detected. In total the formation of **63** accounted for 50% of the radioactivity dosed and 60% of that recovered between 0 and 24 h.

Knowing the identity of the primary route of metabolism, CYP phenotyping was undertaken with recombinant CYP450 isoforms, which revealed that CYPs 1A1 and 1A2 are primarily responsible for the metabolism of **43** (Figure 3a). CYP1A1 is expressed at only very low levels in the liver and is predominantly an extrahepatic CYP, although it can be induced via the aryl hydrocarbon receptor.^{34,35} CYP1A2 is expressed mainly in the liver but is also expressed extrahepatically in rats.^{34,36} Incubations of **43** with CYPs 1A1 and 1A2 revealed that formation of **63** correlated with disappearance of **43**, and only minor levels of the aldehyde **35** were seen in vitro. Knowing that these CYP450 isoforms are expressed extrahepatically, stability

studies were undertaken with microsomes isolated from different organs (Figure 3b), which revealed that **43** was degraded by lung and kidney microsomes in the presence of NADPH, in addition to liver microsomes, with intrinsic clearance of 22, 22, and 28 (μL/min)/mgP. In contrast, **43** was stable in heart microsomes and showed only modest metabolism in intestinal microsomes Cl_{int} = 5 (μL/min)/mgP.

With this information analogues were screened using recombinant CYP1A1; **43**, the dimethylamino **37**, the piperidine **39**, and the isopropyl **47** derivatives were all degraded rapidly, with Cl_{int} = 6, 8.7, 3.8, and 0.8 (μL/min)/mgP. This is in good agreement with the high clearances seen in vivo in rats. On the other hand, the *N*-methylpiperazine derivative **41**, which showed modest stability in RLM, showed improved stability in the presence of CYP1A1 Cl_{int} < 0.1 (μL/min)/mgP, and when this compound was dosed iv to rats, it displayed low plasma clearance Cl = 8 (mL/min)/kg, with long terminal half-life t_{1/2} = 9.7 h.

A strategy to improve the PK properties was to block the methylene group through steric crowding; therefore, the corresponding mono- and *gem*-dimethyl derivatives, **48** and **50**, were prepared. Both compounds maintained PARP inhibitory activity with IC₅₀ = 3.7 and 16 nM, respectively, and were capable of blocking PARP activity in cells as revealed by EC₉₀ = 680 and 900 nM. This level of PARP inhibition resulted in the inhibition of proliferation of BRCA-1 deficient HeLa cells with CC₅₀ = 3.1 and 0.92 μM, respectively, albeit with only a modest selectivity over wild type cells. Both derivatives showed good stability in rat liver microsomes as seen previously with **43**, with **48** and **50** having intrinsic clearances of 9 and 11 (μL/min)/mgP, respectively. The introduction of the steric crowding on the benzylic methylene served to protect these derivatives from oxidation by CYP1A1 as demonstrated by improved stability compared to **43** against this recombinant CYP, with Cl_{int} = 2.2 and 0.4 (μL/min)/mgP for **48** and **50**, respectively. Moreover, this improved stability was recapitulated in vivo where the addition of a single methyl group reduced the rat

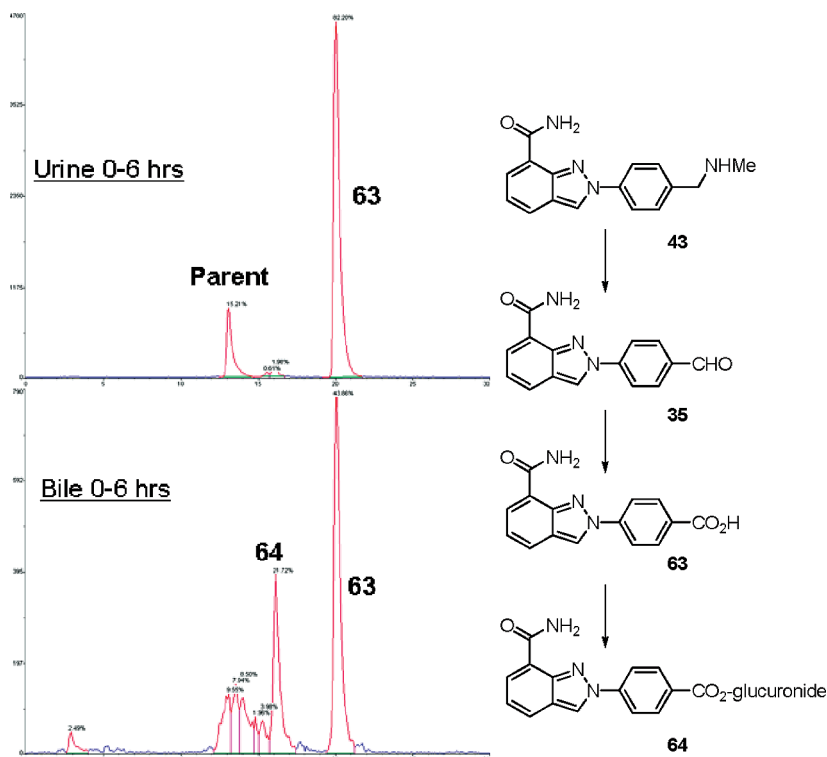


Figure 2. Metabolite profiles were obtained by radiochromatography of urine and bile following dosing of [^3H]43 (300 $\mu\text{Ci}/\text{kg}$).³³ Separation was by RP-HPLC, using a Ace Act RP C18 150 mm \times 2.1 mm column (Mac Mod Analytical Inc., Chadds Ford, PA) coupled to a Packard 515TR radiodetector (Perkin-Elmer Life and Analytical Sciences, Boston, MA) equipped with a 500 μL liquid scintillation flow cell.

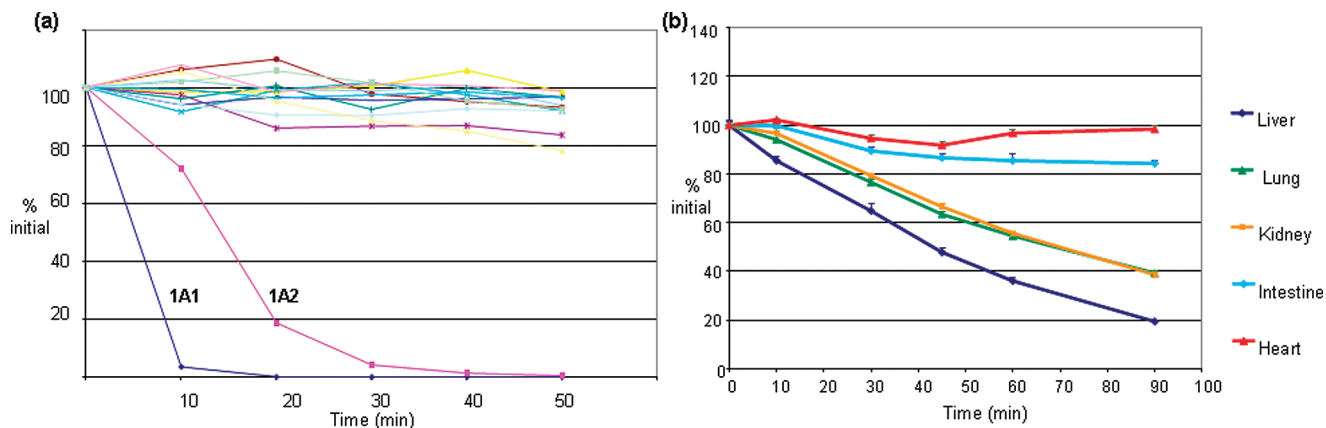


Figure 3. (a) Stability of 43 in the presence of rat rCYP isoforms. (b) Metabolic stability of 43 in liver, lung, kidney, intestine microsomes and heart homogenate in the presence of NADPH.

plasma clearance to 58 (mL/min)/kg, while the *gem*-dimethyl group reduced plasma clearance still further to 30 (mL/min)/kg.

Despite the improvement in PK properties, the activity of these derivatives was still suboptimal, and accordingly attempts were undertaken to increase the activity by restricting the rotational freedom of the amines, either by closing the methylamine back onto the phenyl ring as in **13** and **14** (Table 2) or through cyclization onto the benzylic methylene, as in **15**–**17**. Locking the amine into a tetrahydroisoquinoline system like **13** or **14** resulted in a modest improvement in enzymatic activity, and both analogues displayed around a 2-fold improvement in activity, with $\text{EC}_{90} = 310$ and 140 nM in the PARylation assay and antiproliferative activities of 130 and 270 nM, respectively, in BRCA-1 silenced cells. Both analogues showed excellent selectivity for the BRCA-1

silenced cells, with 16- and 20-fold higher concentrations required to cause antiproliferative effects in wild-type cells. Despite the encouraging profile, **13** was still characterized by high plasma clearance in rats, with $\text{Cl} = 87$ (mL/min)/kg, reflecting the moderate stability in both rat microsomes and CYP1A1, $\text{Cl}_{\text{int}} = 52$ and 0.7 ($\mu\text{L}/\text{min}$)/mgP, respectively. In contrast, the isomer **14** showed slightly better microsomal stability with $\text{Cl}_{\text{int}} = 36$ ($\mu\text{L}/\text{min}$)/mgP, and lower plasma clearance in vivo where $\text{Cl} = 30$ (mL/min)/kg. This compound also displayed modest oral bioavailability, $F = 22\%$.

Unfortunately cellular activity was still suboptimal and efforts focused on the other cyclization strategy (Tables 2 and 3). Accordingly, pyrrolidine **15** and piperidine derivatives **16** and **17** were prepared. These three analogues bore the basic amine at increasing distances from the aromatic

ring. The first two analogues displayed similar enzyme activities, although the piperidine **16** was characterized by 2-fold improvement in cellular activity, with $EC_{90} = 220$ nM in the PARylation assay. This analogue was the first compound from this series to display double digit antiproliferation activity, $CC_{50} = 72$ nM, in BRCA-1 deficient cells and displayed >25-fold selectivity for BRCA-1 silenced cells compared to their wild type counterparts. In contrast, the 4-piperidinyl isomer **17** displayed around a 3-fold weaker enzyme activity, and this was reflected in weaker cellular activity with $CC_{50} = 410$ nM in BRCA-1 deficient cells. Unsurprisingly, the pyrrolidine **15** with the amine in a benzylic position was a substrate of CYP1A1 ($Cl_{int} = 2.5$ ($\mu\text{L}/\text{min}$)/mgP), but the 3-piperidinyl **16** derivative bearing a phenethylamine showed good stability both in rat liver microsomes and in recombinant CYP1A1, $Cl_{int} = 11$ and 0.3 ($\mu\text{L}/\text{min}$)/mgP, respectively. When dosed to rats, **16** displayed moderate plasma clearance $Cl = 47$ (mL/min)/kg and excellent oral bioavailability, $F = 74\%$. The 4-piperidinyl derivative **17** showed similar in vitro properties, but given the weaker cellular activity with BRCA-1, $CC_{50} = 410$ nM.

Table 4. Inhibitory Activity of **56** on Individual PARP Isoform^a

	IC ₅₀ (nM)
PARP-1	3.8
PARP-2	2.1
PARP-3	1300
V-PARP	330
TANK-1	570

^aValues are the mean of at least four experiments (standard deviations were within 25% of the mean values).

Table 5. Antiproliferation Activity of **56**^a

cell line	tumor type	mutation	CC ₅₀ (nM)
MDA-MB-436	mammary gland adenocarcinoma	BRCA1 5396 + 1G > A mutation and loss of wt allele	18
CAPAN-1 cells	pancreas adenocarcinoma	BRCA2 6174delT mutation and loss of wt allele	90
human prostate epithelial			> 5000
human mammary epithelial			> 5000

^aValues are the mean of at least four experiments (standard deviations were within 25% of the mean values).

Given the encouraging properties of **16**, the two enantiomers were separated and profiled, and although only marginal differences in activity between **56** and **57** were seen on the enzyme (PARP-1 IC₅₀ = 3.2 and 2.4 nM, respectively), the *S*-enantiomer **56** proved to be around an order of magnitude more active in cells with $EC_{50} = 4$ nM and $EC_{90} = 45$ nM in the PARylation assay, compared to $EC_{50} = 30$ nM and $EC_{90} = 280$ nM for the enantiomer **57**. Similarly, the *S*-enantiomer **56** displayed improved antiproliferation effects in the BRCA-1 silenced cells with $CC_{50} = 33$ nM, compared to 470 nM for the *R*-enantiomer **57**. As seen previously for the racemate, excellent selectivity was seen between BRCA-1 silenced and wild-type cells with **56** displaying a 23-fold window. The absolute stereochemistry of the piperidine was determined by Mosher's amide analysis (see Supporting Information), as well as through comparison to a synthetic intermediate prepared by nitration and reduction of (*S*)-3-phenylpiperidine prepared by enantioselectively as described by Bosch.³⁷ The pharmacokinetics of the *S*-enantiomer **56** both in vitro and in vivo in rats were slightly inferior to those of the **57**, but nevertheless, **56** was characterized by acceptable pharmacokinetics in rats with plasma clearance of 28 (mL/min)/kg, very high volume of distribution ($V_{d,ss} = 6.9$ L/kg), long terminal half-life ($t_{1/2} = 3.4$ h), and excellent bioavailability, $F = 65\%$.

Given the interest in **56**, it was profiled against several other PARP family members in a trichloroacetic acid precipitation assay looking at the incorporation of [³H]NAD into the growing PAR polymers (Table 4). It was demonstrated to be a potent and selective PARP-1 and PARP-2 inhibitor with IC₅₀ = 3.8 and 2.1 nM, respectively. Furthermore, it displayed at least a 100-fold selectivity over PARP-3, V-PARP, and tankyrase-1, with IC₅₀ = 1300, 330, and

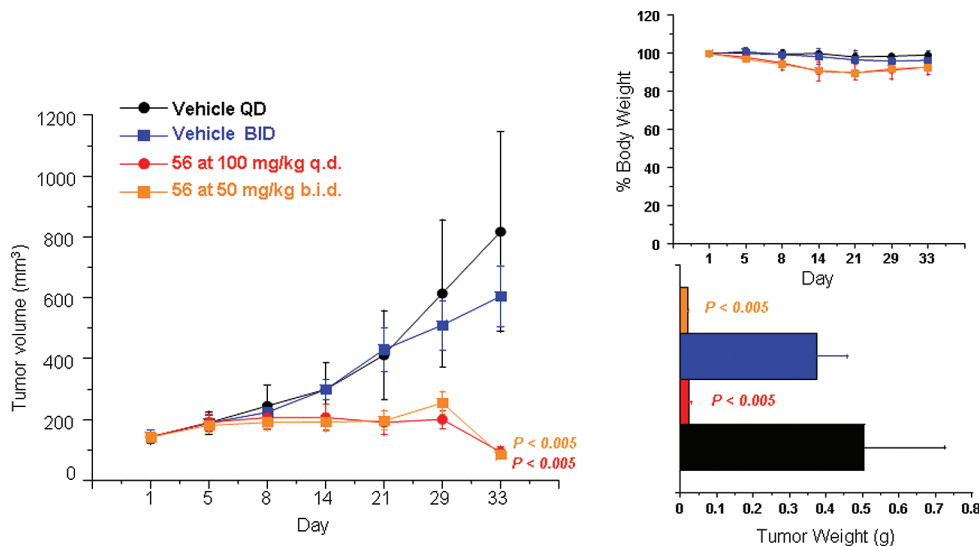


Figure 4. Activity of **56** in MDA-MB-436 (BRCA-1 mutant) xenograft bearing mice when dosed orally at 100 mg/kg q.d. or 50 mg/kg b.i.d. for 33 days. For each group, $n = 7$.

570 nM, respectively. As well as inhibiting the growth of HeLa cell lacking BRCA-1 because of silencing by RNA interference, this derivative is able to inhibit the proliferation of cancer cell lines carrying natural BRCA-1 or BRCA-2 mutations (Table 5). In MDA-MB-436 human mammary gland adenocarcinoma cells carrying BRCA-1 mutations, **56** displayed $CC_{50} = 18$ nM, while in CAPAN-1 human pancreatic adenocarcinoma cells, which are BRCA-2 mutant, **56** displayed $CC_{50} = 90$ nM. The latter result substantiates the evidence that potent PARP inhibitors are capable of killing BRCA-2 deficient cells.³⁸ In contrast, normal human prostate and mammary epithelial cells are resistant to **56**, displaying antiproliferative effects in the micromolar range, thereby demonstrating the very high selective cytotoxicity from these PARP inhibitors in BRCA-1 and -2 mutant cancer cells compared to surrounding tissue.

The in vivo efficacy of the compound was demonstrated preclinically in a BRCA-1 mutant MDA-MB-436 xenograft model (Figure 4), and 2×10^6 cells were injected subcutaneously in the right flank of 6-week-old nude CD1 female mice. When tumors reached an average volume of 150 mm^3 , mice were randomized to form homogeneous groups and treated with **56**, dosing orally at either 100 mg/kg q.d. or 50 mg/kg b.i.d. Tumor regression was observed with both dosing regimes, and both were well tolerated, with no mortality. Less than 10% body weight loss was seen during the experiment.

Further characterization of the preclinical profile of **56** will be described elsewhere in due course, and **56** is currently undergoing clinical evaluation in a phase 1 clinical trial in cancer patients.³⁹

Conclusions

A novel series of 2-phenyl-2*H*-indazole-7-carboxamide PARP inhibitors has been developed. Introduction of a *p*-alkylaminomethyl group improved cellular activity but resulted in detrimental PK properties as a result of oxidation by CYP1A enzymes. Subsequent optimization culminated in the identification of **56** which is a potent and selective PARP 1 and 2 inhibitor, displaying more than 100-fold selectivity over the other PARP family members. This compound has a double digit nanomolar antiproliferative activity on a range of BRCA mutant tumor cells and displays high selectivity over normal epithelial cells. In a mouse xenograft model using BRCA-1 mutant cells, **56** is efficacious at well tolerated doses when administered orally. These preclinical findings have supported the transition of **56** into clinical development.

Experimental Section

General Experimental Details. Solvents and reagents were obtained from commercial suppliers and were used without further purification. HPLC-MS and UPLC-MS analyses were performed on either a Waters Alliance 2795 apparatus or an Acquity UPLC. Nuclear magnetic resonance spectra were obtained on Bruker AMX spectrometers and are referenced in ppm relative to TMS. High resolving power accurate mass measurement electrospray (ES) and atmospheric pressure chemical ionization (APCI) mass spectral data were acquired by use of a Bruker Daltonics 7T Fourier transform ion cyclotron resonance mass spectrometer (FT-ICR MS). All final compounds displayed $\geq 95\%$ purity as determined by analytical RP-HPLC on an Acquity Waters UPLC using three different methods.

PARP-1 SPA Assay. Enzyme assay was conducted in buffer containing 25 mM Tris, pH 8.0, 1 mM DTT, 1 mM spermine, 50 mM KCl, 0.01% Nonidet P-40, and 1 mM MgCl_2 . PARP reactions contained 0.1 μCi [^3H]NAD⁺ (200 000 DPM), 1.5 μM NAD⁺, 150 nM biotinylated NAD⁺, 1 $\mu\text{g}/\text{mL}$ activated calf thymus, and 1–5 nM PARP-1. Autoreactions utilizing SPA bead-based detection were carried out in 50 μL volumes in white 96-well plates.

Compounds were prepared in 11-point serial dilution in 96-well plate, 5 $\mu\text{L}/\text{well}$ in 5% DMSO/ H_2O (10 \times concentrated). Reactions were initiated by adding first 35 μL of PARP-1 enzyme in buffer and incubating for 5 min at room temperature and then 10 μL of NAD⁺ and DNA substrate mixture. After 3 h at room temperature, these reactions were terminated by the addition of 50 μL of streptavidin-SPA beads (2.5 mg/mL in 200 mM EDTA, pH 8). After 5 min, they were counted using a TopCount microplate scintillation counter. IC_{50} data was determined from inhibition curves at various substrate concentrations.

PARP Isoform TCA Assays. The enzymatic reaction was conducted in the presence of 25 mM Tris-HCl pH 8.0, 1 mM MgCl_2 , 50 mM KCl, 1 mM spermine, 0.01% Nonidet P-40, and 1 mM DTT. PARP reactions contained 0.1 μCi [^3H]NAD (200 000 DPM), 1.5 μM NAD⁺, 1 $\mu\text{g}/\text{mL}$ activated calf thymus, and 0.2–1 nM human PARP-1 enzyme. Assays were carried out in 50 μL volumes in white 96-well polypropylene microplate.

A 96-well plate was prepared with serial dilutions over 10 points over a 0.1–50 nM concentration range 5% DMSO/ H_2O , 5 μL . Reactions were initiated by adding first 35 μL of PARP-1 enzyme in buffer and incubating for 5 min at room temperature, then 10 μL of NAD⁺ and DNA substrate mixture. After 2 h incubation at room temperature, the reaction was stopped by the addition of TCA (50 $\mu\text{L}/\text{well}$, 20% in 20 mM NaPPI solution) and incubated for 10 min over ice. The resulting precipitate was filtered on a Unifilter GF/B microplate and washed four times with 2.5% TCA. After addition of 50 $\mu\text{L}/\text{well}$ of scintillation liquid the amount of radioactivity incorporated into the PAR polymers was determined using a TopCount microplate scintillation counter. IC_{50} data were determined from inhibition curves at various substrate concentrations. The protocols for the other PARP family members are very similar with subtle changes as described in the Supporting Information.

PARYlation Assay. HeLa cells were seeded into a 96-well Viewplate black microplate at an initial concentration of 10 000 cells/well in culture medium (100 μL of DMEM containing 10% FCS, 0.1 mg/mL penicillin–streptomycin, and 2 mM L-glutamine). The plates were incubated for 4 h at 37 $^\circ\text{C}$ under 5% CO_2 atmosphere, and then compounds were added with serial dilutions over nine points over a 0.3–100 nM concentration range in 5% DMSO/ H_2O , 10 $\mu\text{L}/\text{well}$. The plate was then incubated for 18 h at 37 $^\circ\text{C}$ in 5% CO_2 , and then DNA damage was provoked by addition of 5 μL of H_2O_2 solution in H_2O (final concentration 200 μM). As a negative control, cells untreated with H_2O_2 were used. The plate was kept at 37 $^\circ\text{C}$ for 5 min. Then the medium was gently removed by plate inversion, and the cells were fixed by addition of ice-cold MeOH (100 $\mu\text{L}/\text{well}$) and kept at -20 $^\circ\text{C}$ for 20 min.

After removal of the fixative by plate inversion and washing 10 times with PBS (300 μL), the detection buffer (100 $\mu\text{L}/\text{well}$, containing PBS, Tween (0.05%), and BSA (1 mg/mL)) together with the primary PAR mAb (Alexis ALX-804-220, 1:2000), the secondary antimouse Alexa Fluor 488 antibody (Molecular Probes A11029, 1:3000), and nuclear dye Draq5 (Alexis Bos 889001R200, 5 μM) were added. Following 3 h incubation at room temperature in the dark, removal of the solution, and washing 10 times with PBS (300 μL), the plate was read on an InCell1000. Monitoring for PAR polymer was by detection of Alexa488 at Ex. S 475_20X, Em. HQ 535_50, exposure time of 600 ms, and identification of the nuclei was by tracking Draq5

with Ex. HQ 620_60X, Em. HQ 700_75M, exposure time of 300 ms. The % PAR-positive cells was calculated by measuring the ratio between the numbers of PAR-positive nuclei over the total number of Draq5-labeled nuclei. The IC₅₀ was determined on the basis of the residual enzyme activity in the presence of increasing PARPi concentration.

Proliferation Assay in BRCA-1 Silenced and Wild Type HeLa Cells. HeLa BRCA1-silenced cells were generated by transducing HeLa cells at an MOI of 100 with a lentivirus containing an H1-derived expression cassette for a shRNA against BRCA-1 and an expression cassette for GFP (GFP under the control of EF1- α promoter). Silencing of BRCA1 was more than 80% as assessed by Taqman analysis. Control BRCA wild type HeLa cells were generated by transducing them with a lentivirus expressing GFP only.

Proliferation assays were conducted in 96-well black view-plates, and 300 cells/well (250 cell/well for BRCA-1 wt) in culture medium, 190 μ L/well (DMEM containing 10% FCS, 0.1 mg/mL penicillin–streptomycin, and 2 mM L-glutamine), were plated and incubated for 4 h at 37 °C under 5% CO₂ atmosphere. Inhibitors were then added with serial dilutions, 10 μ L/well to obtain the desired final compound concentration in 0.5% DMSO. The cells were then incubated for 7 days at 37 °C in 5% CO₂ after which time viability was assessed. Briefly, with CellTiter-Blue (Promega) solution prediluted 1:10 in medium, 100 μ L/well was added and the cells left for 45 min at 37 °C under 5% CO₂ and then a further 15 min at room temperature in the dark. The number of living cells was determined by reading the plate at fluorimeter, excitation at 550 nm and emission at 590 nm. Cell growth was expressed as the percentage growth with respect to vehicle treated cells. The concentration required to inhibit cell growth by 50% (CC₅₀) was determined. The protocols for the other cell lines are very similar and are described in the Supporting Information.

Xenograft Model. The MDA-MB-436 human breast cancer cells (ATCC) were grown in RPMI 1640 medium with L-glutamine supplemented with 10% FCS, penicillin (100 U/mL), and streptomycin (100 μ g/mL) in standard adherent culture conditions at 37 °C and 5% CO₂. For establishment of xenograft tumors, cells were harvested from subconfluent cultures using EDTA/trypsin, washed in serum free-medium, and injected (2 \times 10⁶ cells) subcutaneously in the right flank of 6-week-old nude CD1 female mice in 100 μ L total volume of 1:1 mix of cell suspension in serum-free media and RGF-Matrigel. When tumor reached an average volume of 150 mm³, mice were randomized to form homogeneous groups and treatment started, dosing orally. Mice were dosed orally in water (10 mL/kg) with 100 mg/kg q.d. or 50 mg/kg b.i.d. for 33 days, with tumor growth and body weight measurements done at least once a week.

General Methods for the Synthesis of Indazole PARP Inhibitors. Preparation of Imines 6a–k (Method A). A mixture of methyl 3-formyl-2-nitrobenzoate (**5**) (1.0 equiv) and the corresponding aniline (1.05 equiv) in EtOH (0.2 M) was stirred at reflux under N₂ atmosphere for 2 h until TLC revealed completion of the reaction. Evaporation of the solvent gave a white solid which was used in the next step without further purification.

Preparation of Methyl 2H-Indazole-7-carboxylate Esters 7a–k (Method B). A mixture of the imine (**6a–k**) (1.0 equiv) and NaN₃ (1.05 equiv) in dry DMF (0.3 M) was stirred at 90 °C overnight under N₂ atmosphere. The crude was concentrated under reduced pressure and the residue purified by flash column chromatography on silica.

Preparation of 2H-Indazole-7-carboxamides 8–17 (Method C). A solution of the corresponding carboxylic ester (**7a–k**) in NH₃ (7 N solution in MeOH, 200 equiv) in a sealed tube was heated to 60 °C for 36 h. After the mixture was cooled, solvent was evaporated under reduced pressure and the residue purified by flash column chromatography.

Preparation of Methyl 2-(4-Formylphenyl)-2H-indazole-7-carboxylate 32 (Method D). To a solution of methyl 2H-indazole-7-carboxylate (**31**) (1.0 equiv) in DMF (0.8 M) were added K₂CO₃ (1.1 equiv) and 4-fluorobenzaldehyde (1.3 equiv), and the reaction mixture was heated under microwave conditions at 200 °C for 10 min. The reaction mixture was cooled to room temperature and diluted with EtOAc. The organic phase was washed with brine and dried (Na₂SO₄). Evaporation of the solvent gave (**32**) which was purified by flash column chromatography.

Preparation of Methyl 2-{4-[(Alkylamino)methyl]phenyl}-2H-indazole-7-carboxylate 33a–k (Method E). Methyl 2-(4-formylphenyl)-2H-indazole-7-carboxylate (**32**) (1.0 equiv) was suspended in MeOH (0.1 M), and the amine (8 equiv) was added. To this solution was added a solution of NaBH₃(CN) (1.1 equiv) and ZnCl₂ (0.5 equiv) in MeOH (0.5 mL). The pH was adjusted to 6 with 1.25 M HCl in MeOH, and the mixture stirred at room temperature for 3 h. Then 6 N HCl (0.1 mL) was added and the solvent was reduced in vacuo. Saturated aqueous NaHCO₃ solution was added, the product was extracted with DCM and dried (Na₂SO₄), and the solvents were reduced under reduced pressure.

Methyl 3-Formyl-2-nitrobenzoate (5). To a suspension of 3-methyl-2-nitrobenzoic acid (13.5 g, 74 mmol) in MeOH (200 mL) at 0 °C was added dropwise AcCl (15.9 mL, 224 mmol). The reaction mixture was stirred for 20 h at reflux. The solvent was reduced under reduced pressure, and the residue was dissolved in EtOAc, washed several times with saturated aqueous NaHCO₃ solution and brine, and dried (Na₂SO₄). Evaporation of the solvent gave methyl 3-methyl-2-nitrobenzoate (**4**) (12.4 g, 85%) as a white solid which was used in the next step without further purification. ¹H NMR (400 MHz, CDCl₃, 300 K) δ 7.86 (1H, d, J = 7.5 Hz), 7.53–7.42 (2H, m), 3.89 (3H, s), 2.36 (3H, s). MS (ES) C₉H₉NO₄ requires 195, found 218 (M + Na)⁺.

A mixture of methyl 3-methyl-2-nitrobenzoate (12.4 g, 63.3 mmol), (BzO)₂ (0.92 g, 3.8 mmol), and NBS (13.3 g, 74.7 mmol) in CCl₄ (320 mL) was heated at reflux under N₂ atmosphere for 12 h. The mixture was cooled to room temperature, diluted with DCM, concentrated under reduced pressure while dry loading onto silica gel. The residue was purified by flash column chromatography on silica gel using 10% EtOAc/petroleum ether to yield methyl 3-(bromomethyl)-2-nitrobenzoate (6.94 g, 40%) as a white solid. ¹H NMR (400 MHz, CDCl₃, 300K) δ 7.93 (1H, d, J = 7.7 Hz), 7.72 (1H, d, J = 7.7 Hz), 7.57 (1H, t, J = 7.7 Hz), 4.43 (2H, s), 3.88 (3H, s). MS (ES) C₉H₈BrNO₄ requires 273/275, found 242/244 (M – MeO)⁺, 227/229 (M – NO₂)⁺.

To a mixture of methyl 3-(bromomethyl)-2-nitrobenzoate (6.94 g, 25.3 mmol) and 4 Å molecular sieves (35 g) in MeCN (125 mL) at room temperature was added N-methylmorpholine N-oxide (5.93 g, 50.6 mmol), and the reaction mixture was stirred for 1.5 h under N₂ atmosphere. Then the mixture was diluted with EtOAc and filtered and the filtrate was washed with H₂O, 1 N HCl, brine, and dried (Na₂SO₄). Evaporation of the solvent gave methyl 3-formyl-2-nitrobenzoate (**5**) as a white solid (3.92 g, 74%) which was used in the next step without further purification. ¹H NMR (400 MHz, CDCl₃, 300 K) δ 9.96 (1H, s), 8.26 (1H, d, J = 7.9 Hz), 8.18 (1H, d, J = 7.9 Hz), 7.77 (1H, t, J = 7.9 Hz), 3.93 (3H, s). MS (ES) C₉H₇NO₅ requires 209, found 208 (M – H)[–].

Methyl 2-Nitro-3-[(phenylimino)methyl]benzoate (6a). **6a** was prepared according to general method A, using **5** (0.4 g, 1.9 mmol) and aniline (0.18 g, 2.0 mmol) to afford methyl 2-nitro-3-[(phenylimino)methyl]benzoate (**6a**) which was used in the next step without further purification. ¹H NMR (400 MHz, CDCl₃, 300 K) δ 8.51 (1H, d, J = 7.3 Hz), 8.41 (1H, s), 8.11 (1H, d, J = 7.3 Hz), 7.67 (1H, t, J = 7.8 Hz), 7.43 (2H, t, J = 7.8 Hz), 7.31 (1H, t, J = 7.3 Hz), 7.16 (2H, d, J = 7.8 Hz), 3.94 (3H, s).

Methyl 2-Phenyl-2H-indazole-7-carboxylate (7a). **7a** was prepared according to general method B using **6a** (0.54 g, 1.9 mmol)

to give, after purification by flash column chromatography on silica using a gradient of 10–40% EtOAc/petroleum, ether methyl 2-phenyl-2*H*-indazole-7-carboxylate (**7a**) (0.18 g, 37% over two steps) as a brown oil. ¹H NMR (400 MHz, CDCl₃, 300 K) δ 8.50 (1H, s), 8.12 (1H, d, *J* = 7.0 Hz), 7.96–7.90 (3H, m), 7.49 (2H, t, *J* = 7.6 Hz), 7.38 (1H, t, *J* = 7.4 Hz), 7.15 (1H, t, *J* = 7.4 Hz), 4.03 (3H, s). MS (ES) C₁₅H₁₂N₂O₂ requires 252, found 253 (M + H)⁺.

2-Phenyl-2*H*-indazole-7-carboxamide (8). **8** was prepared according to general method C using **7a** (0.18 g, 0.7 mmol) to afford, after purification by flash column chromatography on silica using a gradient of 30–50% EtOAc/petroleum ether, **8** (47 mg, 28%) as white solid. ¹H NMR (400 MHz, DMSO, 300 K) δ 9.33 (1H, s), 8.56 (1H, br s), 8.16 (2H, d, *J* = 7.9 Hz), 8.08–8.00 (2H, m), 7.88 (1H, br s), 7.63 (2H, t, *J* = 7.7 Hz), 7.50 (1H, t, 7.4 Hz), 7.27 (1H, t, *J* = 7.9 Hz). HRMS (ESI) *m/z* calcd for C₁₄H₁₂N₃O 238.0975, found 238.0977. MS (ES) C₁₄H₁₁N₃O requires 237, found 238 (M + H)⁺.

Methyl 2,3-Diaminobenzoate (19). A mixture of 2-amino-3-nitrobenzoic acid methyl ester (**18**) (6 g, 30 mmol) and Pd/C (0.6 g, 10% w/w) in MeOH (100 mL) was stirred for 3 days at room temperature under H₂ atmosphere (1 atm). The mixture was filtered through Celite, and then the solvent was evaporated under reduced pressure. The red solid of crude methyl 2,3-diaminobenzoate (**19**) (4.88 g, 96%) was used in the next step without further purification. ¹H NMR (300 MHz, CDCl₃, 300 K) δ 7.46 (1H, dd, *J* = 8.1 and 1.4 Hz), 6.84 (1H, dd, *J* = 7.5 and 1.4 Hz), 6.59 (1H, dd, *J* = 8.1 and 7.5 Hz), 3.87 (3H, s). MS (ES) C₈H₁₀N₂O₂ requires 166, found 167 (M + H)⁺.

Methyl 3-Amino-2-[phenyldiazenyl]benzoate (20). A mixture of methyl 2,3-diaminobenzoate (**19**) (400 mg, 2.4 mmol) and nitrosobenzene (284 mg, 2.6 mmol) in AcOH (25 mL) was stirred for 3 h at room temperature. Evaporation of the solvent gave methyl 3-amino-2-[phenyldiazenyl]benzoate (**20**) as a yellow solid which was used in the next step without purification. ¹H NMR (400 MHz, CDCl₃, 300 K) δ 8.00 (1H, dd, *J* = 8.0 and 1.6 Hz), 7.96 (1H, dd, *J* = 7.6 and 1.6 Hz), 7.83 (2H, d, *J* = 7.6 Hz), 7.45–7.35 (4H, m), 6.71 (1H, t, *J* = 8.0 Hz), 3.89 (3H, s). MS (ES⁺) C₁₄H₁₃N₃O₂ requires 255, found 256 (M + H)⁺.

Methyl 2-Phenyl-2*H*-1,2,3-benzotriazole-4-carboxylate (21). A mixture of the crude methyl 3-amino-2-[phenyldiazenyl]benzoate (**20**) (1.2 mmol) and Cu(OAc)₂ (218 mg, 1.2 mmol) in DMF (4.5 mL) was stirred for 90 min at 80 °C while O₂ was bubbled through this solution. The mixture was cooled to room temperature and diluted with EtOAc. The organic phase was washed with brine and dried (Na₂SO₄). Evaporation of the solvent gave methyl 2-phenyl-2*H*-1,2,3-benzotriazole-4-carboxylate (**21**) as a yellow oil which was used in the next step without purification. ¹H NMR (300 MHz, CDCl₃, 300 K) δ 8.45 (1H, d, *J* = 7.8 Hz), 8.29 (2H, d, *J* = 7.2 Hz), 8.17 (2H, d, *J* = 7.8 Hz), 7.41–7.33 (3H, m), 4.05 (3H, s). MS (ES⁺) C₁₄H₁₁N₃O₂ requires 253, found 276 (M + Na)⁺.

2-Phenyl-2*H*-1,2,3-benzotriazole-4-carboxamide (22). A mixture of the crude methyl 2-phenyl-2*H*-1,2,3-benzotriazole-4-carboxylate (**21**) (1.2 mmol) and NaOH (72 mg, 1.8 mmol) in dioxane/water (4:1) (25 mL) was stirred overnight at room temperature. Then 1 N HCl was added until pH 5 was obtained. Evaporation of the solvents under reduced pressure gave the crude carboxylic acid which was dissolved in DMF (5 mL), and HATU (684 mg, 1.8 mmol) was added. After the mixture was stirred for 15 min, DIPEA (0.42 mL, 2.4 mmol) and ammonia (0.5 M in THF, 7.2 mL, 3.6 mmol) were added, and the reaction mixture was stirred for 36 h. The mixture was diluted with EtOAc, and the organic phase was washed with saturated aqueous NaHCO₃ solution and brine and dried. Evaporation of the solvent gave a crude which was purified by preparative RP-HPLC (column, C₁₈), using H₂O (0.1% TFA) and MeCN (+0.1% TFA) as eluents, to afford 2-phenyl-2*H*-1,2,3-benzotriazole-4-carboxamide (**22**) (70 mg, 12% over three steps) as a yellow solid. ¹H NMR (300 MHz, DMSO-*d*₆, 300 K) δ 8.44 (2H,

d, *J* = 7.8 Hz), 8.25 (1H, d, *J* = 8.4 Hz), 8.12 (2H, d, *J* = 7.1 Hz), 8.03 (1H, br s), 7.72–7.56 (4H, m). HRMS (ESI) *m/z* calcd for C₁₃H₁₁N₄O 239.0927, found 239.0929. MS (ES) C₁₃H₁₀N₄O requires 238, found 239 (M + H)⁺.

1-Amino-2-(ethoxycarbonyl)pyridinium 2,4,6-Trimethylbenzenesulfonate (24). Ethyl 2-picolinate (**23**) (500 mg, 3.3 mmol) in DCM (10 mL) was treated with *O*-mesitylenesulfonylhydroxylamine (1.07 g, 5.0 mmol) at room temperature. After 15 min a further portion of *O*-mesitylenesulfonylhydroxylamine (1.07 g, 5.0 mmol) was added and stirring continued for 2 h. The resulting solution was diluted with Et₂O (100 mL) and the resulting precipitate removed by filtration and dried under reduced pressure to yield the desired compound (1.15 g, 95%). ¹H NMR (300 MHz, DMSO-*d*₆, 300 K) δ 8.91 (1H, d, *J* = 5.5 Hz), 8.48 (1H, d, *J* = 5.5 Hz), 8.36 (1H, t, *J* = 5.5 Hz), 8.16 (1H, t, *J* = 5.5 Hz), 6.71 (2H, s), 4.48 (2H, q, *J* = 7.2 Hz), 2.52 (6H, s), 2.29 (3H, s), 1.39 (3H, q, *J* = 7.2 Hz).

Benzyl 7-Carbamoyl-2-phenylpyrazolo[1,5-*a*]pyridine-3-carboxylate (25). 1-Amino-2-(ethoxycarbonyl)pyridinium 2,4,6-trimethylbenzenesulfonate (**24**) (1.15 g, 3.1 mmol), benzyl 3-phenylpropionate (0.74 g, 3.1 mmol), and K₂CO₃ (434 mg, 3.1 mmol) in THF (30 mL) were stirred at room temperature for 18 h. The inorganics were removed by filtration, and the filtrate was concentrated under reduced pressure. The crude residue was dissolved in toluene (50 mL) and heated at reflux for 4 h and then concentrated under reduced pressure and purified by column chromatography on silica eluting with 20% EtOAc/petroleum ether to yield the desired material (**25**) (184 mg, 15%). ¹H NMR (300 MHz, DMSO-*d*₆, 300 K) δ 8.36 (1H, d, *J* = 5.5 Hz), 7.78–7.63 (4H, m), 7.59 (1H, d, *J* = 5.5 Hz), 7.48–7.27 (7H, m), 5.32 (2H, s), 4.47 (2H, q, *J* = 7.2 Hz), 1.19 (3H, t, *J* = 7.2 Hz). MS (ES) C₂₄H₂₀N₂O₄ requires 400 found 401 (M + H)⁺.

Ethyl 2-Phenylpyrazolo[1,5-*a*]pyridine-7-carboxylate (26). The substrate **25** (184 mg, 0.46 mmol) was taken up in EtOH (20 mL) and EtOAc (20 mL) and hydrogenated in the presence of 10% Pd/C (75 mg) under an H₂ atmosphere for 4 h. The catalyst was filtered off and the solvent concentrated under reduced pressure to yield 7-(ethoxycarbonyl)-2-phenylpyrazolo[1,5-*a*]pyridine-3-carboxylic acid (130 mg, 91%). MS (ES) C₁₇H₁₄N₂O₄ requires 310 found 311 (M + H)⁺. The residue (130 mg, 0.42 mmol) was taken up in 48% HBr solution (2 mL) and heated at reflux for 75 min. The reaction mixture was concentrated under reduced pressure azeotroping with toluene, then taken up in MeCN/H₂O and lyophilized. The crude residue (178 mg) was used in the next step without purification. MS (ES) C₁₆H₁₄N₂O₂ requires 266 found 267 (M + H)⁺.

2-Phenylpyrazolo[1,5-*a*]pyridine-7-carboxamide (27). Ethyl 2-phenylpyrazolo[1,5-*a*]pyridine-7-carboxylate (**26**) was converted to 2-phenylpyrazolo[1,5-*a*]pyridine-7-carboxamide according to general method C and then purified by column chromatography on silica eluting with 50% EtOAc/petroleum ether to yield the titled compound (34 mg, 34%) as a white solid. ¹H NMR (300 MHz, DMSO-*d*₆, 300 K) δ 9.38 (1H, s), 8.44 (1H, s), 8.06 (2H, d, *J* = 6.0 Hz), 7.97 (1H, d, *J* = 6.9 Hz), 7.76 (1H, d, *J* = 6.9 Hz), 7.55–7.47 (2H, m), 7.46–7.37 (2H, m), 7.31 (1H, s). HRMS (ESI) *m/z* calcd for C₁₄H₁₂N₃O 238.0975, found 238.0976. MS (ES) C₁₄H₁₁N₃O requires 237 found 238 (M + H)⁺.

Methyl 2-Phenyl[1,2,4]triazolo[1,5-*a*]pyridine-8-carboxylate (29). *O*-Mesitylenesulfonylhydroxylamine (236 mg, 1.1 mmol) was added to a stirred solution of methyl 2-aminopyridine-3-carboxylate (**28**) (152 mg, 1 mmol) in dioxane (10 mL) at room temperature. The reaction mixture was stirred at room temperature for 2 h. Then benzaldehyde (134 μL, 1.3 mmol) was added and the reaction mixture was heated to reflux for 2 h. After the mixture was cooled, KOH (1 N in MeOH, 1 mL, 1 mmol) was added and the resulting dark-brown mixture was stirred at room temperature overnight. The reaction mixture was diluted with H₂O and extracted with EtOAc. The combined organic phase was dried (Na₂SO₄). Evaporation of the solvent under reduced

pressure gave methyl 2-phenyl[1,2,4]triazolo[1,5-*a*]pyridine-8-carboxylate (**29**) as a brown oil which was used in the next step without further purification. ¹H NMR (400 MHz, DMSO-*d*₆, 300 K) δ 9.25 (1H, d, *J* = 6.4 Hz), 8.28 (1H, d, *J* = 7.2 Hz), 9.25 (2H, dd, *J* = 8.0 and 2.0 Hz), 7.94–7.89 (2H, m), 7.31 (2H, d, *J* = 5.6 Hz), 3.97 (3H, s). MS (ES) C₁₄H₁₁N₃O₂ requires 253, found 254 (M + H)⁺.

2-Phenyl[1,2,4]triazolo[1,5-*a*]pyridine-8-carboxamide (30). Methyl 2-phenyl[1,2,4]triazolo[1,5-*a*]pyridine-8-carboxylate (**29**) (1 mmol) was converted according to method C to give 2-phenyl[1,2,4]triazolo[1,5-*a*]pyridine-8-carboxamide (**30**) (63 mg, 26% over two steps) as a white solid. ¹H NMR (400 MHz, DMSO-*d*₆, 300 K) δ 9.20 (1H, d, *J* = 6.0 Hz), 8.96 (1H, br s), 8.33–8.28 (3H, m), 8.21 (1H, br s), 7.60–7.55 (3H, m), 7.38 (1H, t, *J* = 7.2 Hz). HRMS (ESI) *m/z* calcd for C₁₃H₁₁N₄O 239.0927, found 239.0928. MS (ES) C₁₃H₁₀N₄O requires 238, found 239 (M + H)⁺.

Methyl 2-(4-Formylphenyl)-2H-indazole-7-carboxylate (32). **32** was prepared according to general method D using methyl 2H-indazole-7-carboxylate (**31**) (0.3 g, 1.7 mmol) and 4-fluorobenzaldehyde (235 μL, 2.2 mmol) to give, after purification by flash column chromatography on silica using a gradient of 30–40% EtOAc/petroleum ether, methyl 2-(4-formylphenyl)-2H-indazole-7-carboxylate (**32**) (185 mg, 39%). ¹H NMR (400 MHz, CDCl₃, 300 K) δ 10.08 (1H, s), 8.64 (1H, s), 8.20 (2H, d, *J* = 8.6 Hz), 8.16 (1H, d, *J* = 7.2 Hz), 8.05 (2H, d, *J* = 8.6 Hz), 7.96 (1H, d, *J* = 7.2 Hz), 7.21 (1H, t, *J* = 7.2 Hz), 4.06 (3H, s). MS (ES) C₁₆H₁₂N₂O₃ requires 280, found 281 (M + H)⁺.

2-(4-Formylphenyl)-2H-indazole-7-carboxamide (35). **35** was prepared according to general method D using 2H-indazole-7-carboxamide (**34**) (0.8 g, 5.0 mmol) and 4-fluorobenzaldehyde (685 μL, 6.4 mmol) to yield, after purification by flash column chromatography on silica with 10% MeOH/DCM, 2-(4-formylphenyl)-2H-indazole-7-carboxamide (**35**) (0.59 g, 45%). ¹H NMR (400 MHz, DMSO-*d*₆, 300 K) δ 10.10 (1H, s), 9.50 (1H, s), 8.52 (1H, br s), 8.45 (2H, d, *J* = 8.6 Hz), 8.15 (2H, d, *J* = 8.6 Hz), 8.08 (1H, d, *J* = 7.2 Hz), 8.04 (1H, d, *J* = 7.2 Hz), 7.92 (1H, br s), 7.30 (1H, t, *J* = 7.2 Hz). MS (ES) C₁₅H₁₁N₃O₂ requires 265, found 266 (M + H)⁺.

2-(4-Acetylphenyl)-2H-indazole-7-carboxamide (36). **36** was prepared following general method D using 2H-indazole-7-carboxamide (**34**) (322 mg, 2 mmol) and 1-(4-fluorophenyl)ethanone (0.19 mL, 2 mmol). The product (**36**) (540 mg, 97%) was obtained as a white solid by precipitation from the reaction mixture by adding MeOH/EtOAc (5:1) and was used in the next step without further purification. ¹H NMR (400 MHz, DMSO-*d*₆, 300 K) δ 9.48 (1H, s), 8.53 (1H, br s), 8.36 (2H, d, *J* = 8.8 Hz), 8.20 (2H, d, *J* = 8.8 Hz), 8.09 (1H, dd, *J* = 7.0 and 0.8 Hz), 8.05 (1H, dd, *J* = 8.4 and 0.8 Hz), 7.92 (1H, br s), 7.30 (1H, dd, *J* = 8.4 and 7.0 Hz), 2.66 (3H, s). MS (ES⁺) C₁₆H₁₃N₃O₂ requires 279, found 280 (M + H)⁺.

2-{4-[(Dimethylamino)methyl]phenyl}-2H-indazole-7-carboxamide (37). **37** was prepared according to general method E, with methyl 2-(4-formylphenyl)-2H-indazole-7-carboxylate (**32**) (50 mg, 0.18 mmol) and 2.0 M Me₂NH in MeOH (0.71 mL, 1.4 mmol) to give methyl 2-{4-[(dimethylamino)methyl]phenyl}-2H-indazole-7-carboxylate (**33a**) which was used in the next step without further purification. MS (ES) C₁₈H₁₉N₃O₂ requires 309, found 310 (M + H)⁺. Methyl 2-{4-[(dimethylamino)methyl]phenyl}-2H-indazole-7-carboxylate (**33a**) (55 mg, 0.18 mmol) was treated according to general method C to give, after purification by flash column chromatography on silica with 10% MeOH/DCM, 2-{4-[(dimethylamino)methyl]phenyl}-2H-indazole-7-carboxamide (**37**) (40 mg, 76%). ¹H NMR (300 MHz, CD₃CN, 300 K) δ 8.85 (1H, s), 8.78 (1H, br s), 8.17 (1H, d, *J* = 8.0 Hz), 8.05–8.00 (3H, m), 7.56 (2H, d, *J* = 8.4 Hz), 7.28 (1H, t, *J* = 8.0 Hz), 6.36 (1H, br s), 3.56 (2H, s), 2.28 (6H, s). HRMS (ESI) *m/z* calcd for C₁₇H₁₉N₄O 295.1553, found 295.1554. MS (ES) C₁₇H₁₈N₄O requires 294, found 295 (M + H)⁺.

{4-[7-(Aminocarbonyl)-2H-indazol-2-yl]phenyl}-N-methylmethanaminium Chloride (43). Methyl 2-{4-[(methylamino)methyl]-

phenyl}-2H-indazole-7-carboxylate (**33g**) was prepared according to general method E using methyl 2-(4-formylphenyl)-2H-indazole-7-carboxylate (**32**) (80 mg, 0.28 mmol) and MeNH₂·HCl (308 mg, 4.6 mmol) in a mixture DCE/MeOH (4:1, 5 mL), and AcOH was used to adjust the pH to 6. The crude product was used in the next step without further purification. MS (ES) C₁₇H₁₇N₃O₂ requires 295, found 296 (M + H)⁺. 2-{4-[(Methylamino)methyl]phenyl}-2H-indazole-7-carboxamide was prepared according to general method C using methyl 2-{4-[(methylamino)methyl]phenyl}-2H-indazole-7-carboxylate (**33g**). The residue was purified by flash column chromatography on silica using a gradient of 0–20% DCM/MeOH (+1% Et₃N) to afford a yellow powder (62 mg, 78%). The free base (21 mg, 0.08 mmol) was then dissolved in a solution of CH₃CN/H₂O (1:1, 0.025 M), concentrated HCl (81 μL, 0.08 mmol) was added and the solution was lyophilized, affording **43** (23 mg, quant) as a yellow powder. ¹H NMR (400 MHz, DMSO-*d*₆, 300 K) δ 9.30 (1H, s), 9.26 (2H, br s), 8.47 (1H, br s), 8.19 (2H, d, *J* = 8.4 Hz), 8.00 (1H, d, *J* = 6.8 Hz), 7.96 (1H, d, *J* = 8.2 Hz), 7.81 (1H, br s), 7.71 (2H, d, *J* = 8.4 Hz), 7.21 (1H, app t, *J* = 7.6 Hz), 4.14 (2H, s), 2.43 (3H, s). HRMS (ESI) *m/z* calcd for C₁₆H₁₇N₄O 281.1397, found 281.1403. MS (ES) C₁₆H₁₆N₄O requires 280, found 281 (M + H)⁺.

1-{4-[7-(Aminocarbonyl)-2H-indazol-2-yl]phenyl}-N-methylethanaminium Chloride (48). **48** was prepared according to general method E using 2-(4-acetylphenyl)-2H-indazole-7-carboxamide (**36**) (0.1 g, 0.36 mmol) which, after purification by IST ISOLUTE SPE column SCX, gave 2-{4-[1-(methylamino)ethyl]phenyl}-2H-indazole-7-carboxamide (78 mg, 74%). The free base (78 mg, 0.26 mmol) was then dissolved in a solution of CH₃CN/H₂O (1:1) and 37% HCl_(aq) (0.26 mmol) and the solution was lyophilized, affording 1-{4-[7-(aminocarbonyl)-2H-indazol-2-yl]phenyl}-N-methylethanaminium chloride (**48**) as a yellow powder. ¹H NMR (400 MHz, DMSO-*d*₆, 300 K) δ 9.79 (1H, br s), 9.43–9.38 (1H, m), 9.38–9.35 (1H, m), 8.55 (1H, s), 8.26 (1H, d, *J* = 8.4 Hz), 8.07 (1H, d, *J* = 6.8 Hz), 8.03 (2H, d, *J* = 8.2 Hz), 7.88 (1H, br s), 7.81 (2H, d, *J* = 8.2 Hz), 7.28 (1H, app t, *J* = 7 Hz), 4.44–4.40 (1H, m), 2.42 (3H, s), 1.62 (3H, d, *J* = 6.8 Hz). HRMS (ESI) *m/z* calcd for C₁₇H₁₉N₄O 295.1553, found 295.1556. MS (ES⁺) C₁₇H₁₈N₄O requires 294, found 295 (M + H)⁺.

2-[4-(1-Hydroxy-1-methylethyl)phenyl]-2H-indazole-7-carboxamide (49). To a solution of 2-(4-acetylphenyl)-2H-indazole-7-carboxamide (**36**) (2.0 g, 7.2 mmol) in THF (150 mL) at 0 °C, MeMgBr (3 M in THF, 3.6 mL, 10.7 mmol) was added dropwise. The mixture was stirred overnight at room temperature, then quenched with H₂O and extracted with EtOAc. The combined organic phase was dried over MgSO₄. Evaporation of the solvent under reduced pressure gave 2-[4-(1-hydroxy-1-methylethyl)phenyl]-2H-indazole-7-carboxamide (**49**) (1.6 g, 76%) as a yellow solid. ¹H NMR (400 MHz, DMSO-*d*₆, 300 K) δ 9.27 (1H, s), 8.57 (1H, br s), 8.07–8.00 (4H, m), 7.87 (1H, br s), 7.68 (2H, d, *J* = 8.6 Hz), 7.28–7.24 (1H, m), 1.48 (6H, s). MS (ES⁺) C₁₇H₁₇N₃O₂ requires 295, found 296 (M + H)⁺.

2-{4-[7-(Aminocarbonyl)-2H-indazol-2-yl]phenyl}-N-methylpropan-2-aminium Trifluoroacetate (50). In a well ventilated fume hood, to a solution of 2-[4-(1-hydroxy-1-methylethyl)phenyl]-2H-indazole-7-carboxamide (**49**) (0.5 g, 1.7 mmol) and NaCN (0.41 g, 8.5 mmol) in DCM (10 mL) was added concentrated H₂SO₄ (0.45 mL, 8.5 mmol), and the mixture was stirred for 24 h at room temperature. The reaction mixture was quenched by addition of saturated aqueous NaHCO₃ solution, and the mixture was extracted with EtOAc. The combined organic phase was dried (MgSO₄) and evaporation of the solvent under reduced pressure gave a residue that was purified by flash chromatography column using 0–10% MeOH/DCM to afford 2-{4-[1-(formylamino)-1-methylethyl]phenyl}-2H-indazole-7-carboxamide (120 mg, 22%) as a yellow solid. ¹H NMR (600 MHz, DMSO-*d*₆, 300 K) δ 9.27 (1H, s), 8.57 (1H, br s), 8.43 (1H, br s), 8.07–8.01 (4H, m), 7.99 (1H, d, *J* = 1.6 Hz), 7.88 (1H, br s), 7.57 (2H, d, *J* = 8.6 Hz), 7.26 (1H, dd,

$J = 8.1$ and 7.0 Hz), 1.61 (6H, s). MS (ES⁺) C₁₈H₁₈N₄O₂ requires 322, found 323 (M + H)⁺.

To a solution of 2-[4-[1-(formylamino)-1-methylethyl]phenyl]-2H-indazole-7-carboxamide (60 mg, 0.19 mmol) in THF (6 mL) was added BH₃·THF (1 M in THF, 0.28 mL, 0.28 mmol), and the mixture was stirred for 24 h at room temperature. Then saturated aqueous NaHCO₃ solution was added and the mixture was extracted with EtOAc. The combined organic phase was dried over MgSO₄. Evaporation of the solvent under reduced pressure gave a residue that was purified by RP-HPLC (column, C₁₈), using H₂O (0.1% TFA) and MeCN (+0.1% TFA) as eluents, to afford 2-[4-[7-(aminocarbonyl)-2H-indazol-2-yl]phenyl]-N-methylpropan-2-aminium trifluoroacetate (**50**) (8 mg, 10%) as a yellow solid. ¹H NMR (400 MHz, DMSO-*d*₆, 300 K) δ 9.38 (s, 1H), 9.14 (1H, br s), 8.53 (1H, br s), 8.27 (2H, d, $J = 8.7$ Hz), 8.08–8.01 (2H, m), 7.88 (1H, br s), 7.79 (2H, d, $J = 8.7$ Hz), 7.28 (1H, t, $J = 8.2$ Hz), 2.36 (3H, s), 1.73 (6H, s). HRMS (ESI) m/z calcd for C₁₈H₂₁N₄O 309.1710, found 309.1712. MS (ES⁺) C₁₈H₂₀N₄O requires 308, found 309 (M + H)⁺.

Methyl 2-[4-[1-(tert-Butoxycarbonyl)piperidin-3-yl]phenyl]-2H-indazole-7-carboxylate (7i). **7i** was prepared following the general methods A and B using methyl 3-formyl-2-nitrobenzoate (**5**) (1.0 g, 4.8 mmol) and *N*-Boc-3-(4-aminophenyl)piperidine (1.45 g, 5.3 mmol). The crude residue was purified by flash column chromatography on silica using a gradient of 20–40% EtOAc/petroleum ether to yield the desired **7i** (0.95 g, 46%) as a yellow solid. ¹H NMR (400 MHz, CDCl₃, 300 K) δ 8.51 (1H, s), 8.13 (1H, d, $J = 7.1$ Hz), 7.95 (1H, d, $J = 8.3$ Hz), 7.91 (2H, d, $J = 8.4$ Hz), 7.39 (2H, d, $J = 8.4$ Hz), 7.18 (1H, app t, $J = 7.2$ Hz), 4.30–4.10 (2H, m), 4.00 (3H, s), 2.85–2.70 (3H, m), 2.11–2.03 (1H, m), 1.83–1.75 (1H, m), 1.73–1.53 (2H, m), 1.48 (9H, s). MS (ES) C₂₅H₂₉N₃O₄ requires 435, found 436 (M + H)⁺.

tert-Butyl 3-[4-[7-(Aminocarbonyl)-2H-indazol-2-yl]phenyl]piperidine-1-carboxylate (55). The title compound was prepared according to general method C from **7i** (0.95 g, 2.18 mmol), and the crude product was purified by trituration with Et₂O to give the desired product (**55**) (0.75 g, 82%) as a yellow solid. ¹H NMR (400 MHz, CDCl₃, 300 K) δ 9.04 (1H, br s), 8.51 (1H, s), 8.31 (1H, d, $J = 6.8$ Hz), 7.91 (1H, d, $J = 8.3$ Hz), 7.84 (2H, d, $J = 8.2$ Hz), 7.42 (2H, d, $J = 8.2$ Hz), 7.31–7.22 (1H, m), 5.95 (1H, br s), 4.40–4.05 (2H, m), 2.90–2.70 (3H, m), 2.15–2.00 (1H, m), 1.85–1.75 (1H, m), 1.75–1.50 (2H, m), 1.48 (9H, s). MS (ES) C₂₄H₂₈N₄O₃ requires 420, found 421 (M + H)⁺.

3-[4-[7-(Aminocarbonyl)-2H-indazol-2-yl]phenyl]piperidinium Chloride (16). To a stirred solution of *tert*-butyl 3-[4-[7-(aminocarbonyl)-2H-indazol-2-yl]phenyl]piperidine-1-carboxylate (**55**) (0.75 g, 1.78 mmol) in EtOAc (8.9 mL) was added HCl (4 N in dioxane, 6.67 mL, 26.7 mmol), and the reaction mixture was stirred at room temperature for 3 h. Solvent was evaporated under reduced pressure and the crude product purified by trituration with Et₂O to yield the desired (**16**) (0.59 g, 93%) as a yellow solid. ¹H NMR (400 MHz, DMSO-*d*₆, 300 K) δ 9.32 (1H, s), 9.12 (1H, br s), 8.87 (1H, br s), 8.55 (1H, br s), 8.13 (2H, d, $J = 8.6$ Hz), 8.06 (1H, d, $J = 7.0$ Hz), 8.02 (1H, d, $J = 8.4$ Hz), 7.89 (1H, br s), 7.55 (2H, d, $J = 8.6$ Hz), 7.27 (1H, dd, $J = 8.4$ and 7.0 Hz), 3.43–3.27 (2H, m), 3.17–3.03 (2H, m), 3.00–2.85 (1H, m), 2.00–1.70 (4H, m). HRMS (ESI) m/z calcd for C₁₉H₂₁N₄O 321.1710, found 321.1720. MS (ES) C₁₉H₂₀N₄O requires 320, found 321 (M + H)⁺.

(3R)-3-[4-[7-(Aminocarbonyl)-2H-indazol-2-yl]phenyl]piperidinium Chloride (57) and (3S)-3-[4-[7-(Aminocarbonyl)-2H-indazol-2-yl]phenyl]piperidinium Chloride (56). The racemate **16** was separated by chiral SFC purification using CO₂ as supercritical eluent: column, Chiralpak AS-H, 1 mm × 25 mm.; flow = 10 mL/min; $T_{\text{col}} = 35$ °C; $P_{\text{col}} = 100$ bar; modifier, 55% ⁱPrOH containing 4% Et₂NH. Retention time of the first eluting enantiomer was 4.80 min. Evaporation of the solvent followed by lyophilization gave 2-[4-[(3R)-piperidin-3-yl]phenyl]-2H-indazole-7-carboxamide as a white powder (99.0% ee). Retention time of the

second eluting enantiomer was 6.51 min. Evaporation of the solvent followed by lyophilization gave 2-[4-[(3S)-piperidin-3-yl]phenyl]-2H-indazole-7-carboxamide as a white powder (99.2% ee). ¹H NMR (400 MHz, DMSO-*d*₆, 300 K) δ 9.28 (1H, s), 8.57 (1H, br s), 8.06 (2H, d, $J = 7.2$ Hz), 8.04 (2H, d, $J = 8.4$ Hz), 7.88 (1H, br s), 7.49 (2H, d, $J = 8.4$ Hz), 7.27 (1H, dd, $J = 8.4$, 7.2 Hz), 3.08–2.94 (2H, m), 2.77–2.67 (1H, m), 2.64–2.52 (1H, m), 1.98–1.90 (1H, m), 1.75–1.47 (4H, m). MS (ES) C₁₉H₂₀N₄O requires 320, found 321 (M + H)⁺. The chlorohydrate salts of both enantiomers were prepared by stirring a solution of the free base in 1 N HCl for 15 min and lyophilization of the resulting solution, affording the corresponding hydrochloride salts as a pale-yellow solids.

(3R)-3-[4-[7-(Aminocarbonyl)-2H-indazol-2-yl]phenyl]piperidinium Chloride (57). [α]_D²⁰ +133.3 (*c* 0.004, MeOH). HRMS (ESI) m/z calcd for C₁₉H₂₁N₄O 321.1710, found 321.1711.

(3S)-3-[4-[7-(Aminocarbonyl)-2H-indazol-2-yl]phenyl]piperidinium Chloride (56). [α]_D²⁰ –137.9 (*c* 0.004, MeOH). ¹H NMR (600 MHz, DMSO-*d*₆, 300 K) δ 9.32 (1H, s), 9.30 (1H, br d, $J = 10.7$ Hz), 9.10 (1H, dt, $J = 10.7$, 10.3 Hz), 8.56 (1H, br s), 8.13 (2H, d, $J = 8.5$ Hz), 8.06 (1H, dd, $J = 7.0$, 0.8 Hz), 8.02 (1H, dd, $J = 8.3$, 0.8 Hz), 7.90 (1H, br s), 7.55 (2H, d, $J = 8.5$ Hz), 7.27 (1H, dd, $J = 8.3$, 7.0 Hz), 3.35–3.29 (2H, m), 3.16–3.06 (2H, m), 2.92 (1H, m), 1.95–1.74 (4H, m). ¹³C NMR (150 MHz, DMSO-*d*₆, 300 K) δ 165.5, 146.1, 142.2, 138.2, 129.7, 128.5, 125.3, 123.5, 123.4, 121.9, 121.5, 120.9, 47.5, 42.8, 38.7, 29.4, 22.1. HRMS (ESI) m/z calcd for C₁₉H₂₁N₄O 321.1710, found 321.1712. MS (ES) C₁₉H₂₀N₄O requires 320, found 321 (M + H)⁺.

Alternative preparation of (3S)-3-[4-[7-(Aminocarbonyl)-2H-indazol-2-yl]phenyl]piperidinium Chloride (56). **3-(4-Nitrophenyl)pyridine (59)**. A mixture of 1-iodo-4-nitrobenzene (40.6 g, 0.16 mol) and pyridine-3-boronic acid (30 g, 0.24 mmol) in THF (0.82 L) together with 2 M solution Na₂CO₃ (0.24 L) was degassed with a stream of N₂ for 1 h. Pd(PPh₃)₄ (9.5 g, 8.2 mmol) was added, and the reaction mixture was heated at reflux for 72 h. After the mixture was cooled, solvents were concentrated and then EtOAc (500 mL) was added. The aqueous phase was separated and extracted with DCM (2 × 250 mL). The combined organic phase was dried (Na₂SO₄) and solvent evaporated, giving a residue that was purified by flash chromatography column on silica gel 20–100% EtOAc/petroleum ether. The solid obtained after evaporation of the solvent was recrystallized in EtOH and filtered to give 3-(4-nitrophenyl)pyridine (**59**) (23.2 g, 71%) as a pale-beige solid. ¹H NMR (400 MHz, CDCl₃, 300 K) δ 8.87 (1H, s), 8.69 (1H, d, $J = 4.6$ Hz), 8.34 (2H, d, $J = 8.4$ Hz), 7.95 (1H, d, $J = 8.0$ Hz), 7.74 (2H, d, $J = 8.4$ Hz), 7.46 (1H, dd, $J = 8.0$, 4.6 Hz). MS (ES) C₁₁H₈N₂O₂ requires 200, found 201 (M + H)⁺.

4-Piperidin-3-ylaniline (60). PtO₂ (0.5 g) was added to a solution of 3-(4-nitrophenyl)pyridine (**59**) (5 g, 25 mmol) and HCl (1.0 N solution in water, 25 mL, 25 mmol) in MeOH (250 mL). The reaction mixture was stirred for 24 h at room temperature under H₂ atmosphere (50 psi) in a Parr hydrogenation apparatus. The mixture was filtered through Celite, and then the solvent was evaporated under reduced pressure. The resulting white solid was dissolved in EtOAc (250 mL) and washed with 1 N NaOH (100 mL). The aqueous phase was extracted with EtOAc (3 × 250 mL), and the combined organic phase was dried (Na₂SO₄). Evaporation of the solvent gave 4-piperidin-3-ylaniline (**60**) (4.27 g, 97%) as a white solid. ¹H NMR (400 MHz, CDCl₃, 300 K) δ 6.98 (2H, d, $J = 8.0$ Hz), 6.61 (2H, d, $J = 8.0$ Hz), 3.55 (2H, br s), 3.15–3.09 (2H, m), 3.15–3.09 (3H, m), 1.98–1.91 (1H, m), 1.79–1.75 (1H, m), 1.66–1.52 (2H, m). MS (ES) C₁₁H₁₆N₂ requires 176, found 177 (M + H)⁺.

(3S)-3-(4-Aminophenyl)piperidinium (2R,3R)-3-Carboxy-2,3-dihydroxypropanoate (61). To a solution of 4-piperidin-3-ylaniline (**60**) (19.2 g, 0.109 mol) in EtOH (4.0 L) was added a 1.0 M solution of L-tartaric acid in EtOH (109 mL, 0.109 mol) over 5 min. Upon addition of the final 20 mL a precipitate started to

form. The mixture was heated to reflux and then left to cool to room temperature and allowed to stand for 2 days. The resulting crystals (21.7 g) were filtered off and dried. Three recrystallizations from EtOH upgraded this material to 8.83 g (24.8%) of (3*S*)-3-(4-aminophenyl)piperidinium (2*R*,3*R*)-3-carboxy-2,3-dihydroxypropanoate (**61**) with > 82% ee. Enantiomeric excess was determined by SFC on semiprep system: column, Chiralpak AD-H (1 cm × 25 cm); flow, 10 mL/min; modifier, gradient from (MeOH + 0.2% DEA) 20% (1 min) to 20% (5.7 min) to 60% to 60% (2 min); $T_{\text{col}} = 35\text{ }^{\circ}\text{C}$; $P_{\text{col}} = 100\text{ bar}$; retention time for desired enantiomer, 4.6 min; retention time for minor enantiomer, 5.2 min.

***tert*-Butyl (3*S*)-3-(4-Aminophenyl)piperidine-1-carboxylate (**62**).** A solution of Boc₂O (4.62 g, 21.2 mmol) in DCM (20 mL) was added dropwise (10 min) to a stirred suspension of (3*S*)-3-(4-aminophenyl)piperidinium (2*R*,3*R*)-3-carboxy-2,3-dihydroxypropanoate (**61**) (6.3 g, 19.3 mmol) in DCM (80 mL) at 0 °C. The reaction mixture was stirred at 0 °C for 40 min. Then a solution of 7 N NH₃ in MeOH (8 mL) was added and the mixture was stirred for 30 min at 0 °C. After dilution with DCM (250 mL) the organic phase was washed with saturated aqueous NaHCO₃ (2 × 250 mL) and dried (Na₂SO₄). Evaporation of the solvent gave *tert*-butyl (3*S*)-3-(4-aminophenyl)piperidine-1-carboxylate (**62**) (4.9 g, 92%) as a white foam which was used in the next step without further purification. ¹H NMR (400 MHz, CDCl₃, 300 K) δ 7.02 (2H, d, $J = 8.0\text{ Hz}$), 6.65 (2H, d, $J = 8.0\text{ Hz}$), 4.23–4.06 (2H, m), 3.65–3.48 (1H, m), 2.74–2.50 (3H, m), 2.00–1.92 (1H, m), 1.78–1.59 (1H, m), 1.64–1.52 (3H, m), 1.46 (9H, s). MS (ES) C₁₆H₂₄N₂O₂ requires 276, found 277 (M + H⁺).

Methyl 2-{4-[(3*S*)-1-(*tert*-Butoxycarbonyl)piperidin-3-yl]phenyl}-2H-indazole-7-carboxylate (7k**).** A mixture of methyl 3-formyl-2-nitrobenzoate (**5**) (3.5 g, 16.9 mmol) and *tert*-butyl (3*S*)-3-(4-aminophenyl)piperidine-1-carboxylate (**62**) (4.9 g, 17.7 mmol) in EtOH (85 mL) was stirred at reflux under N₂ atmosphere overnight until TLC revealed completion of the reaction (petroleum ether/EtOAc = 4:1). Evaporation of the solvent gave *tert*-butyl (3*S*)-3-[4-((1*E*)-[3-(methoxycarbonyl)-2-nitrophenyl]methylene)amino]phenyl]piperidine-1-carboxylate (**6k**) as an oil which was used in the next step without further purification. ¹H NMR (400 MHz, DMSO-*d*₆, 300 K) δ 8.54 (1H, s), 8.36 (1H, dd, $J = 7.8, 1.3\text{ Hz}$), 8.14 (1H, dd, $J = 7.8, 1.3\text{ Hz}$), 7.89 (1H, t, $J = 7.8\text{ Hz}$), 7.33 (2H, d, $J = 8.4\text{ Hz}$), 7.23 (2H, d, $J = 8.4\text{ Hz}$), 4.00–3.90 (2H, m), 3.87 (3H, s), 2.91–2.59 (3H, m), 1.88 (1H, m), 1.73–1.40 (3H, m), 1.39 (9H, s).

NaN₃ (1.1 g, 17.7 mmol) was added to a solution of crude *tert*-butyl (3*S*)-3-[4-((1*E*)-[3-(methoxycarbonyl)-2-nitrophenyl]methylene)amino]phenyl]piperidine-1-carboxylate (**6k**) (16.9 mmol) in dry DMF (68 mL). The reaction mixture was heated at 90 °C for 3 days under N₂ atmosphere. The solvent was removed under reduced pressure and the residue purified by flash column chromatography on silica gel with 20–30% EtOAc/petroleum ether to yield methyl 2-{4-[(3*S*)-1-(*tert*-butoxycarbonyl)piperidin-3-yl]phenyl}-2H-indazole-7-carboxylate (**7k**) (3.4 g, 46% over two steps) as a yellow solid. ¹H NMR (400 MHz, CDCl₃, 300 K) δ 8.51 (1H, s), 8.13 (1H, d, $J = 7.1\text{ Hz}$), 7.95 (1H, d, $J = 8.3\text{ Hz}$), 7.91 (2H, d, $J = 8.4\text{ Hz}$), 7.39 (2H, d, $J = 8.4\text{ Hz}$), 7.18 (1H, app t, $J = 7.2\text{ Hz}$), 4.30–4.10 (2H, m), 4.00 (3H, s), 2.85–2.70 (3H, m), 2.11–2.03 (1H, m), 1.83–1.75 (1H, m), 1.73–1.53 (2H, m), 1.48 (9H, s). MS (ES) C₂₅H₂₉N₃O₄ requires 435, found 436 (M + H⁺).

***tert*-Butyl (3*S*)-3-{4-[7-(Aminocarbonyl)-2H-indazol-2-yl]phenyl}piperidine-1-carboxylate (**63**).** A solution of methyl 2-{4-[(3*S*)-1-(*tert*-butoxycarbonyl)piperidin-3-yl]phenyl}-2H-indazole-7-carboxylate (**7k**) (3.4 g, 7.8 mmol) in 7 N NH₃ in MeOH (195 mL, 1.37 mol) was heated to 60 °C in a sealed tube for 2 days. The solvents were reduced under reduced pressure and the residue purified by flash column chromatography on silica gel 30–80% EtOAc/petroleum ether to yield *tert*-butyl (3*S*)-3-{4-[7-(aminocarbonyl)-2H-indazol-2-yl]phenyl}piperidine-1-carboxylate (**63**) (2.36 g, 72%) as a yellow solid. ¹H NMR

(400 MHz, CDCl₃, 300 K) δ 9.04 (1H, br s), 8.51 (1H, s), 8.31 (1H, d, $J = 6.8\text{ Hz}$), 7.91 (1H, d, $J = 8.3\text{ Hz}$), 7.84 (2H, d, $J = 8.2\text{ Hz}$), 7.42 (2H, d, $J = 8.2\text{ Hz}$), 7.31–7.22 (1H, m), 5.95 (1H, br s), 4.40–4.05 (2H, m), 2.90–2.70 (3H, m), 2.15–2.00 (1H, m), 1.85–1.75 (1H, m), 1.75–1.50 (2H, m), 1.48 (9H, s). MS (ES) C₂₄H₂₈N₄O₃ requires 420, found 421 (M + H⁺).

(3*S*)-3-{4-[7-(Aminocarbonyl)-2H-indazol-2-yl]phenyl}piperidinium Chloride (56**).** HCl (4 N in 1,4-dioxane, 13.7 mL, 55 mmol) was added to a stirred solution of *tert*-butyl (3*S*)-3-{4-[7-(aminocarbonyl)-2H-indazol-2-yl]phenyl}piperidine-1-carboxylate (**63**) (2.3 g, 5.5 mmol) in EtOAc (27.5 mL) at room temperature. The reaction mixture was stirred at room temperature for 3 h. Solvent was evaporated under reduced pressure and the crude product purified by trituration with Et₂O to yield (3*S*)-3-{4-[7-(aminocarbonyl)-2H-indazol-2-yl]phenyl}piperidinium chloride (1.92 g, 98%) as a yellow solid (91% ee).

Acknowledgment. The authors thank Anna Alfieri, Maria Verdirame, and Fabio Bonelli for analytical support, and Fabrizio Fiore and Massimo Aquilina for routine PK studies.

Supporting Information Available: Additional experimental procedures for the biological assays including protocols for the PARP isoforms and proliferation assays in additional cell lines; general experimental details for the chemistry procedures including synthetic procedures for compounds **9–15**, **17**, **38–42**, **44–47**, **52**, and **54**; purity analysis results of the final compounds; and Mosher's amide analysis of the stereochemistry of **56**. This material is available free of charge via the Internet at <http://pubs.acs.org>.

References

- (1) (a) Hassa, P. O.; Hottiger, M. O. The diverse biological roles of mammalian PARPs, a small but powerful family of poly-ADP-ribose polymerases. *Front. Biosci.* **2008**, *13*, 3046–3082. (b) Amé, J.-C.; Spenlehauer, C.; de Murcia, G. The PARP superfamily. *BioEssays* **2004**, *26*, 882–893. (c) Kleine, H.; Poreba, E.; Lesniewicz, K.; Hassa, P. O.; Hottiger, M. O.; Litchfield, D. W.; Shilton, B. H.; Lüscher, B. Substrate-assisted catalysis by PARP10 limits its activity to mono-ADP-ribosylation. *Mol. Cell* **2008**, *32*, 57–69.
- (2) Jagtap, P.; Szabó, C. Poly(ADP-ribose) polymerase and the therapeutic effects of its inhibitors. *Nat. Rev. Drug Discovery* **2005**, *4*, 421–440.
- (3) Schreiber, V.; Dantzer, F.; Amé, J.-C.; de Murcia, G. Poly(ADP-ribose): novel functions for an old molecule. *Nat. Rev. Mol. Cell Biol.* **2006**, *7*, 517–528.
- (4) Huber, A.; Bai, P.; de Murcia, J. M.; de Murcia, G. PARP-1, PARP-2 and ATM in the DNA damage response: functional synergy in mouse development. *DNA Repair* **2004**, *3*, 1103–1108.
- (5) Durkacz, B. W.; Omidiji, O.; Gray, D. A.; Shall, S. (ADP-ribose)_n participates in DNA excision repair. *Nature (London)* **1980**, *283*, 593–596.
- (6) de Murcia, J. M.; Niedergang, C.; Trucco, C.; Ricoul, M.; Dutrillaux, B.; Mark, M.; Oliver, F. J.; Masson, M.; Dierich, A.; LeMeur, M.; Walzinger, C.; Chambon, P.; de Murcia, G. Requirement of poly(ADP-ribose) polymerase in recovery from DNA damage in mice and in cells. *Proc. Natl. Acad. Sci. U.S.A.* **1997**, *94*, 7303–7307.
- (7) Wang, Z.-Q.; Auer, B.; Stingl, L.; Berghammer, H.; Haidacher, D.; Schweiger, M.; Wagner, E. F. Mice lacking ADPRT and poly(ADP-ribosylation) develop normally but are susceptible to skin disease. *Genes Dev.* **1995**, *9*, 509–520.
- (8) Tentori, L.; Graziani, G. Chemopotentiation by PARP inhibitors in cancer therapy. *Pharmacol. Res.* **2005**, *52*, 25–33.
- (9) Rodon, J.; Iniesta, M. D.; Papadopoulos, K. Development of PARP inhibitors in oncology. *Expert Opin. Invest. Drugs* **2009**, *18*, 31–43.
- (10) Ratnam, K.; Low, J. A. Current development of clinical inhibitors of poly(ADP-ribose) polymerase in oncology. *Clin. Cancer Res.* **2007**, *13*, 1383–1388.
- (11) (a) Peukert, S.; Schwahn, U. New inhibitors of poly(ADP-ribose) polymerase (PARP). *Expert Opin. Ther. Pat.* **2004**, *14*, 1531–1551. (b) Alarcon de la Lastra, C.; Villegas, I.; Sanchez-Fidalgo, S. Poly(ADP-ribose) polymerase inhibitors: new pharmacological

- functions and potential clinical implications. *Curr. Pharm. Des.* **2007**, *13*, 933–962.
- (12) Moroni, F. Poly(ADP-ribose)polymerase 1 (PARP-1) and postischemic brain damage. *Curr. Opin. Pharmacol.* **2008**, *8*, 96–103.
- (13) Szabó, C. Cardioprotective effects of poly(ADP-ribose) polymerase inhibition. *Pharmacol. Res.* **2005**, *52*, 34–43.
- (14) Cuzzocrea, S. Shock, inflammation and PARP. *Pharmacol. Res.* **2005**, *52*, 72–82.
- (15) Pacher, P.; Szabó, C. Role of poly(ADP-ribose) polymerase 1 (PARP-1) in cardiovascular diseases: the therapeutic potential of PARP inhibitors. *Cardiovasc. Drug Rev.* **2007**, *25*, 235–260.
- (16) Kauppinen, T. M.; Swanson, R. A. The role of poly(ADP-ribose) polymerase-1 in CNS disease. *Neuroscience (Amsterdam)* **2007**, *145*, 1267–1272.
- (17) Bryant, H. E.; Schultz, N.; Thomas, H. D.; Parker, K. M.; Flower, D.; Lopez, E.; Kyle, S.; Meuth, M.; Curtin, N. J.; Helleday, T. Specific killing of BRCA2-deficient tumours with inhibitors of poly(ADP-ribose) polymerase. *Nature (London)* **2005**, *434*, 913–917.
- (18) Farmer, H.; McCabe, N.; Lord, C. J.; Tutt, A. N. J.; Johnson, D. A.; Richardson, T. B.; Santarosa, M.; Dillon, K. J.; Hickson, I.; Knights, C.; Martin, N. M. B.; Jackson, S. P.; Smith, G. C. M.; Ashworth, A. Targeting the DNA repair defect in BRCA mutant cells as a therapeutic strategy. *Nature (London)* **2005**, *434*, 917–921.
- (19) McCabe, N.; Turner, N. C.; Lord, C. J.; Kluzek, K.; Bialkowska, A.; Swift, S.; Giavara, S.; O'Connor, M. J.; Tutt, A. N.; Zdzienicka, M. Z.; Smith, G. C. M.; Ashworth, A. Deficiency in the repair of DNA damage by homologous recombination and sensitivity to poly(ADP-ribose) polymerase inhibition. *Cancer Res.* **2006**, *66*, 8109–8115.
- (20) (a) Venkitaraman, A. R. Cancer susceptibility and the functions of BRCA1 and BRCA2. *Cell* **2002**, *108*, 171–182. (b) Narod, S. A.; Foulkes, W. D. BRCA1 and BRCA2: 1994 and beyond. *Nat. Rev. Cancer* **2004**, *4*, 665–676.
- (21) Menear, K. A.; Adcock, C.; Boulter, R.; Cockcroft, X.-L.; Copsey, L.; Cranston, A.; Dillon, K. J.; Drzewiecki, J.; Garman, S.; Gomez, S.; Javaid, H.; Kerrigan, F.; Knights, C.; Lau, A.; Loh, V. M., Jr.; Matthews, I. T. W.; Moore, S.; O'Connor, M. J.; Smith, G. C. M.; Martin, N. M. B. 4-[3-(4-Cyclopropanecarbonyl)piperazine-1-carbonyl]-4-fluorobenzyl]-2H-phthalazin-1-one: a novel bioavailable inhibitor of poly(ADP-ribose) polymerase-1. *J. Med. Chem.* **2008**, *51*, 6581–6591.
- (22) Rottenberg, S.; Jaspers, J. E.; Kersbergen, A.; van der Burg, E.; Nygren, A. O. H.; Zander, S. A. L.; Derksen, P. W. B.; de Bruin, M.; Zevenhoven, J.; Lau, A.; Boulter, R.; Cranston, A.; O'Connor, M. J.; Martin, N. M. B.; Borst, P.; Jonkers, J. High sensitivity of BRCA1-deficient mammary tumors to the PARP inhibitor AZD2281 alone and in combination with platinum drugs. *Proc. Natl. Acad. Sci. U.S.A.* **2008**, *105*, 17079–17084.
- (23) Fong, P. C.; Boss, D. S.; Yap, T. A.; Tutt, A.; Wu, P.; Mergui-Roelvink, M.; Mortimer, P.; Swaisland, H.; Lau, A.; O'Connor, M. J.; Ashworth, A.; Carmichael, J.; Kaye, S. B.; Schellens, J. H. M.; de Bono, J. S. Inhibition of poly(ADP-ribose)polymerase in tumors from BRCA mutation carriers. *N. Engl. J. Med.* **2009**, *361*, 123–134.
- (24) (a) Penning, T. D.; Zhu, G.-D.; Gandhi, V. B.; Gong, J.; Liu, X.; Shi, Y.; Klinghofer, V.; Johnson, E. F.; Donawho, C. K.; Frost, D. J.; Bontcheva-Diaz, V.; Bouska, J. J.; Osterling, D. J.; Olson, A. M.; Marsh, K. C.; Luo, Y.; Giranda, V. L. Discovery of the poly(ADP-ribose) polymerase (PARP) inhibitor 2-[(R)-2-methylpyrrolidin-2-yl]-1H-benzimidazole-4-carboxamide (ABT-888) for the treatment of cancer. *J. Med. Chem.* **2009**, *52*, 514–523. (b) Donawho, C. K.; Luo, Y.; Luo, Y.; Penning, T. D.; Bauch, J. L.; Bouska, J. J.; Bontcheva-Diaz, V. D.; Cox, B. F.; DeWeese, T. L.; Dillehay, L. E.; Ferguson, D. C.; Ghoreishi-Haack, N. S.; Grimm, D. R.; Guan, R.; Han, E. K.; Holley-Shanks, R. R.; Hristov, B.; Idler, K. B.; Jarvis, K.; Johnson, E. F.; Kleinberg, L. R.; Klinghofer, V.; Lasko, L. M.; Liu, X.; Marsh, K. C.; McGonigal, T. P.; Meulbroek, J. A.; Olson, A. M.; Palma, J. P.; Rodriguez, L. E.; Shi, Y.; Stavropoulos, J. A.; Tsurutani, A. C.; Zhu, G.-D.; Rosenberg, S. H.; Giranda, V. L.; Frost, D. J. ABT-888, an orally active poly(ADP-ribose) polymerase inhibitor that potentiates DNA-damaging agents in preclinical tumor models. *Clin. Cancer Res.* **2007**, *13*, 2728–2737.
- (25) Thomas, H. D.; Calabrese, C. R.; Batey, M. A.; Canan, S.; Hostomsky, Z.; Kyle, S.; Maegley, K. A.; Newell, D. R.; Skaltzky, D.; Wang, L.-Z.; Webber, S. E.; Curtin, N. J. Preclinical selection of a novel poly(ADP-ribose) polymerase inhibitor for clinical trial. *Mol. Cancer Ther.* **2007**, *6*, 945–956.
- (26) Mason, K. A.; Valdecanaas, D.; Hunter, N. R.; Milas, L. INO-1001, a novel inhibitor of poly(ADP-ribose) polymerase, enhances tumor response to doxorubicin. *Invest. New Drugs* **2008**, *26*, 1–5.
- (27) Kopetz, S.; Mita, M. M.; Mok, I.; Sankhala, K. K.; Moseley, J.; Sherman, B. M.; Bradley, C. R.; Tolcher, A. W. First in Human Phase I Study of BSI-201, a Small Molecule Inhibitor of Poly ADP-ribose Polymerase (PARP) in Subjects with Advanced Solid Tumors. Presented at the 44th Annual Meeting of the ASCO, Chicago, IL, May 31–June 3 **2008**; Abstract 3577. *J. Clin. Oncol.* **2008**, *26* (May 20 Suppl.), 3577.
- (28) Kuvshinov, A. M.; Gulevskaya, V. I.; Rozhkov, V. V.; Shevelev, S. A. Synthesis of 2-substituted 4,6-dinitro-2H-indazoles from 2,4,6-trinitrotoluene. *Synthesis* **2000**, *10*, 1474–1478.
- (29) Anderson, P. L.; Hasak, J. P.; Kahle, A. D.; Paoletta, N. A.; Shapiro, M. J. 1,3-Dipolar addition of pyridine *N*-imine to acetylenes and the use of carbon-13 NMR in several structural assignments. *J. Heterocycl. Chem.* **1981**, *18*, 1149–1152.
- (30) Hajos, G.; Timari, G.; Messmer, A.; Zagyva, A.; Miskolczi, I.; Schantl, J. G. A new synthesis of the *s*-triazolo[1,5-*a*]pyridine ring system. *Monatsh. Chem.* **1995**, *126*, 1213–1215.
- (31) Ritter, J. J.; Kalish, J. α,α -Dimethyl- β -phenethylamine. *Org. Synth.* **1964**, *44*, 44.
- (32) (a) Ruf, A.; Mennissier de Murcia, J.; de Murcia, G.; Schulz, G. E. Structure of the catalytic fragment of poly(AD-ribose) polymerase from chicken. *Proc. Natl. Acad. Sci. U.S.A.* **1996**, *93*, 7481–7485. (b) Ruf, A.; de Murcia, G.; Schulz, G. E. Inhibitor and NAD⁺ binding to poly(ADP-ribose) polymerase as derived from crystal structures and homology modeling. *Biochemistry* **1998**, *37*, 3893–3900.
- (33) [³H]43 was prepared by reduction of {4-[7-(aminocarbonyl)-3-bromo-2H-indazol-2-yl]-2-chlorophenyl}-*N*-methylmethanaminium trifluoroacetate. The precursor itself was prepared from **35** first by reaction with 2-chloro-4-fluorobenzaldehyde and then bromination at the 3-position with Br₂ in DCM/AcOH for 48 h, followed by reductive amination.
- (34) Martignoni, M.; Groothuis, G. M. M.; de Kanter, R. Species differences between mouse, rat, dog, monkey and human CYP-mediated drug metabolism, inhibition and induction. *Expert Opin. Drug Metab. Toxicol.* **2006**, *2*, 875–894.
- (35) Harrigan, J. A.; McGarrigle, B. P.; Sutter, T. R.; Olson, J. R. Tissue specific induction of cytochrome P450 (CYP) 1A1 and 1B1 in rat liver and lung following in vitro (tissue slice) and in vivo exposure to benzo(a)pyrene. *Toxicol. in Vitro* **2006**, *20*, 426–438.
- (36) Ma, Q.; Lu, A. Y. H. CYP1A induction and human risk assessment: an evolving tale of in vitro and in vivo studies. *Drug Metab. Dispos.* **2007**, *35*, 1009–1016.
- (37) Amat, M.; Cantó, M.; Llor, N.; Escolano, C.; Molins, E.; Espinosa, E.; Bosch, J. Dynamic kinetic resolution of racemic γ -aryl- δ -oxoesters. Enantioselective synthesis of 3-arylpiperidines. *J. Org. Chem.* **2002**, *67*, 5343–5351.
- (38) McCabe, N.; Lord, C. J.; Tutt, A. N.; Martin, N. M.; Smith, G. C.; Ashworth, A. BRCA2-deficient CAPAN-1 cells are extremely sensitive to the inhibition of poly(ADP-ribose) polymerase: an issue of potency. *Cancer Biol. Ther.* **2005**, *4*, 934–936.
- (39) MK4827 in Patients with Advanced Solid Tumors and BRCA Mutant Ovarian Cancer. <http://clinicaltrials.gov/ct2/show/NCT00749502>.